

University of Alberta

Chemical-Enhanced Filtration of Cu/Ni Concentrate

by

Haijun Zheng

A thesis submitted to the Faculty of Graduate Studies and Research
in partial fulfillment of the requirements for the degree of

Master of Science

Department of Chemical and Materials Engineering

©Haijun Zheng
Spring 2010
Edmonton, Alberta

Permission is hereby granted to the University of Alberta Libraries to reproduce single copies of this thesis and to lend or sell such copies for private, scholarly or scientific research purposes only. Where the thesis is converted to, or otherwise made available in digital form, the University of Alberta will advise potential users of the thesis of these terms.

The author reserves all other publication and other rights in association with the copyright in the thesis and, except as herein before provided, neither the thesis nor any substantial portion thereof may be printed or otherwise reproduced in any material form whatsoever without the author's prior written permission.

Examining Committee

Zhenghe Xu, Chemical and Materials Engineering

Qingxia, Liu, Chemical and Materials Engineering (Chair)

Tong Yu, Civil and Environmental Engineering

Rajender Gupta, Chemical and Materials Engineering

ABSTRACT

Filtration performance of mineral concentrate is mainly controlled by solid particle size and surface hydrophobicity. Filtration of coarser particles with more hydrophobic surfaces produces better filtration performance characterized by higher filtration rate (U) and lower final moisture content (FMC) in the final cake. Some filtration aids could improve filtration performance by flocculating solid particles and enhancing surface hydrophobicity. For the mineral concentrate used in this study, many filtration aids tested could only improve either U or FMC: one type was effective in improving U, and another type was effective in improving FMC. The combination of the two types of filtration aids at certain dosages could achieve better filtration performance than the optimum performance achieved by each individual filtration aid. Based on the experimental results, the working mechanism of filtration aids behind the filtration behavior was explored to deepen the understanding of the chemical-enhanced filtration of Cu/Ni concentrate.

ACKNOWLEDGEMENTS

I would like to express my great appreciation to my supervisor Dr. Zhenghe Xu for his support and guidance throughout the course of completing this thesis. My sincere appreciation extends to the chair and the members of my examination committee, Dr. Qingxia Liu, Dr. Tong Yu, and Dr. Rajender Gupta, for their helpful criticism and suggestions concerning my thesis.

My great gratitude should be given to Professor Liangjun Zhang, Dr. Wangxi Zhu, Dr. Xianhua Feng, Dr. Trong Dang-Vu, Ms. Xiaoyan Wang, and the oil sands group members for their assistance.

I would like to thank the technical staff in the Department of Chemical and Materials Engineering of University of Alberta.

The financial support for this study from Vale-Inco and technical input by Dr. Tao Xue at Vale-Inco technical services are also greatly appreciated.

Finally, I would like to thank my parents and my family for their understanding, encouragement and support.

TABLE OF CONTENTS

CHAPTER 1. INTRODUCTION	1
CHAPTER 2. LITERATURE REVIEW	9
2.1. Review of Filtration and Dewatering Theories.....	10
2.1.1. Distinction between Filtration and Dewatering.....	10
2.1.2. Filtration and Dewatering Theories	11
2.2. Review of Filtration and Dewatering Practices	13
2.2.1. Coagulants	13
2.2.2. Surfactants	14
2.2.3. Polymer Flocculants	16
CHAPTER 3. FUNDAMENTALS.....	19
CHAPTER 4. EXPERIMENTS.....	25
4.1. Experimental Setup.....	25
4.2. Experimental Materials.....	29
4.3. Instrument and Equipment.....	31
4.4. Filtration Test Procedure	32
4.5. Experimental Procedure	32
4.5.1. Surface Charge of Original Concentrate.....	33
4.5.2. Correlation between Settling and Filtration Performance	34
4.5.3. Filtration Test.....	36

4.5.4. Process Optimization	37
4.5.5. Sample Zeta Potential Measurement	38
4.5.6. Particle Size Distribution Measurement	38
4.5.7. Effects of the Addition of Filtration Aids on Filtrate Viscosity ...	39
4.5.8. Effects of the Addition of Filtration Aids on Surface Tension	40
4.5.9. Saturated Cake Porosity and Permeability Measurement.....	41
4.5.10. Initial Contact Angle Measurement.....	43
4.5.11. Backwashing with Surfactants	44
CHAPTER 5. RESULTS AND DISCUSSION.....	46
5.1. Surface Charge of Original Concentrate	46
5.2. Correlation between Settling and Filtration Performance.....	47
5.2.1. A100	47
5.2.2. MF.....	50
5.2.3. A100 and MF.....	52
5.3. Process Optimization.....	55
5.4. Zeta Potential Measurement	59
5.5. Particle Size Distribution Measurement	60
5.6. Effects of the Addition of Filtration Aids on Filtrate Viscosity	62
5.7. Effects of the Addition of Filtration Aids on Surface Tension	63
5.8. Saturated Cake Porosity and Permeability Measurement	64

5.9. Initial Contact Angle Measurement	66
5.10. Backwashing	67
5.11. Filtration Aid Working Mechanism	69
5.11.1. Working Mechanism: A100	69
5.11.2. Working Mechanisms: MF	71
5.11.3. Working Mechanism: A100 and MF	72
CHAPTER 6. CONCLUSIONS	75
CHAPTER 7. RECOMMENDATIONS	77
BIBLOGRAPHY	78
APPENDICES	80
1. Filtration Test Procedure	80
1.1. Sample Preparation	80
1.2. Conditioning	80
1.3. Computer Workstation	81
1.4. Sample Treatment	82
2. Results	83
3. Filtration Curves	85
4. Table of Test Points	90

LIST OF TABLES

Table 1.	Sample Composition (Wt % on Dry Basis, pH = 12)	29
Table 2.	Composition (AAS) of Supernatant (ppm)	29
Table 3.	Filtration Aids Used in This Study	31
Table 4.	Experimental Conditions	32
Table A2.1.	Original Concentrate Zeta Potential Measurement	83
Table A2.2.	A100 and MF Settling Result	83
Table A2.3.	Zeta Potential Measurement with Filtration Aids.....	83
Table A2.4.	Filtration Test Result	84
Table A2.5.	Interaction Effect Test Result	84
Table A2.6.	Backwashing Result	84
Table A4.1.	Settling Test Points	90
Table A4.2.	Filtration Test Points.....	90

LIST OF FIGURES

Figure 1. Schematic of Filtration Operation	2
Figure 2. Illustration of the Filtration Setup	3
Figure 3. Schematic Illustration of a Filtration Process.....	19
Figure 4. Distinction of Filtration Stages.....	21
Figure 5. Overview of the Experimental Program.....	25
Figure 6. Determination of U.....	27
Figure 7. Determination of FMC	28
Figure 8. Determination of ISR	35
Figure 9. Zeta Potential of Original Concentrate.....	46
Figure 10. Effects of A100 Addition on Settling Performance	48
Figure 11. ISR - U with A100 Addition	48
Figure 12. ISR - SMC with A100 Addition	49
Figure 13. Effects of MF Addition on Settling Performance	50
Figure 14. ISR - U with MF Addition.....	51
Figure 15. ISR - SMC with MF Addition	52
Figure 16. Effects of A100 and MF Addition on Settling Performance	53
Figure 17. ISR - U with A100 and MF Addition	53
Figure 18. ISR - SMC with A100 and MF Addition.....	54
Figure 19. SMC – FMC with A100 and MF Addition.....	56

Figure 20. FMC - U with x g/t A100 + y g/t MF Addition	57
Figure 21. Effects of Filtration Aids Addition on Zeta Potential	60
Figure 22. d_{50} of Sample with Filtration Aids Addition.....	61
Figure 23. Effect of 350 g/t A100 Addition on Filtrate Viscosity	62
Figure 24. Effect of 5.5 g/t MF Addition on Filtrate Viscosity.....	63
Figure 25. U - k_s of Sample with A100 and MF Addition	64
Figure 26. ϵ - k_s of Sample with A100 and MF Addition	65
Figure 27. Initial Contact Angle with A100 and MF Addition	67
Figure 28. FMC of Cake Backwashing with 7.5 g/t DAH Addition.....	68
Figure 29. Working Mechanism of A100.....	70
Figure 30. Working Mechanism of MF.....	71
Figure 31. Working Mechanism of A100 + MF.....	72
Figure 32. Working Mechanism of MF + A100.....	72
Figure A3.1. U with A100 Addition.....	85
Figure A3.2. SMC with A100 Addition	85
Figure A3.3. U with MF Addition.....	86
Figure A3.4. SMC with MF Addition	86
Figure A3.5. U with A100 & MF Addition	87
Figure A3.6. SMC with A100 & MF Addition	87
Figure A3.7. U of x g/t A100 + 5.5 g/t MF Addition	88
Figure A3.8. FMC of x g/t A100 + 5.5 g/t MF Addition.....	88

Figure A3.9. U of 350 g/t A100 + y g/t MF Addition	89
Figure A3.10. FMC of 350 g/t A100 + y g/t MF Addition.....	89
Figure A3.11. Moisture Content Curve of Cake Backwashing with 7.5 g/t DAH Addition.....	90

LIST OF NOMENCLATURES

A - Filtration area

A100 - Aerodri 100

D - Empirical constant

DAH - Dodecylamine Hydrochloride

FMC - Final moisture content

L - Length of capillary/thickness of cake

M - Mass of slurry

MF - Magnafloc 1011

M_f - Mass of filtrate

S - Moisture content in cake

SF - Saturated filtrate

SMC - Saturated moisture content

U - Filtration rate

V - Cumulative volume of filtrate at time t

k - Cake permeability

k_s - Saturated cake permeability

m - Mass of filtrate

p - Filtration pressure

p_c - Capillary pressure

r - Radius of capillary

sc - Solid content

x g/t A + y g/t B - Filtration aid A at dosage x g/t is added at first,
filtration aid B at dosage y g/t is added second

γ - Surface tension of the filtrate

ε - Porosity

ζ - Zeta potential

η - Dynamic viscosity of filtrate

θ - Contact angle of the solid particle

ρ - Density

Δp - Pressure drop across the capillary

CHAPTER 1. INTRODUCTION

In mineral processing, ground raw ores are commonly beneficiated to increase the metal content in the concentrates for subsequent pyrometallurgical or hydrometallurgical processing. Froth flotation is a widely used effective beneficiation method. During flotation, a large amount of water is introduced into the process to form slurries suitable for flotation separation. In general, mineral concentrates in the form of flotation froth contain 25-65% water (Yoon, et al, 2004). The contained water needs to be removed before the concentrate is processed in the smelter. This water removal process is completed through filtration followed by thermal drying: filtration dewateres the concentrate to certain moisture content, and thermal drying further reduces the moisture content to the desired level.

The energy intensive drying process in the metallurgical industry incurs high energy consumption and green house gas emissions, which is a major challenge for every natural resource based-industry. The development of an efficient dewatering process for mineral processing industry will address this challenge. Efficient filtration process, characterized by high filtration rate and low moisture content in the final filter cake, reduces the load to thermal dryers before the mineral solids are sent to smelting furnace, decreasing the energy consumption

and green house gas emissions.

During the filtration process as schematically shown in Figure 1, a cake is formed from the solid particles in the concentrate with the liquid flowing out of the cake. Filtration efficiency is evaluated by two parameters: filtration rate (U) and final moisture content (FMC) in the filter cake (Xu, et al, 1995), the former characterizes how fast the liquid is removed, and the latter characterizes the quality of the final filter cake measured by residual moisture content.

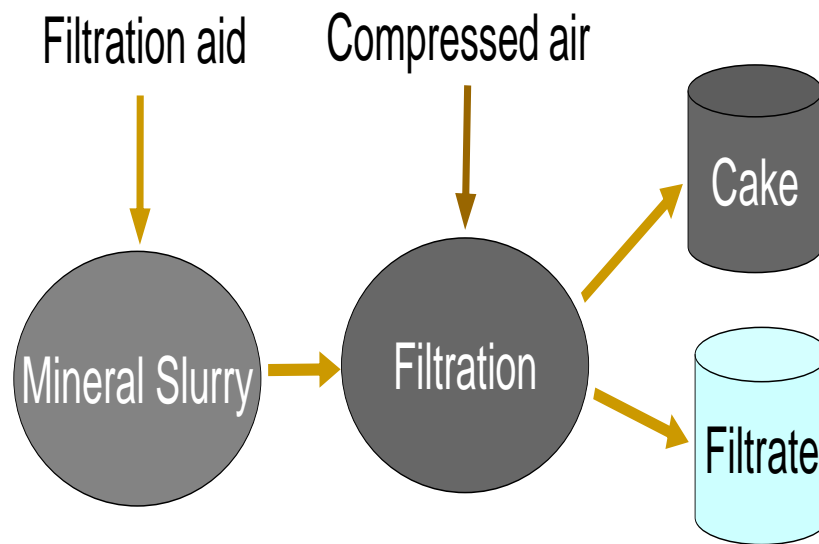


Figure 1. Schematic of Filtration Operation

Filtration process is often modeled as filtrate being forced through a bundle of capillary channels within the cake by external forces such as pressure and vacuum (Svarovsky, 1977). Established filtration theories, represented by Darcy law, Brownell-Katz equation, and Laplace-Young equation, suggest that for a given

process condition, cake permeability, surface tension, and solid surface hydrophobicity are the controlling parameters practical to be manipulated to improve filtration rate and final moisture content (Yu, 1998).

In a typical filtration test, filter press is used to conduct the test. The amount of filtrate passing through the filter cake is recorded as a function of time to produce a typical filtration curve as shown in Figure 2. Based on this curve, many other meaningful results could be generated.

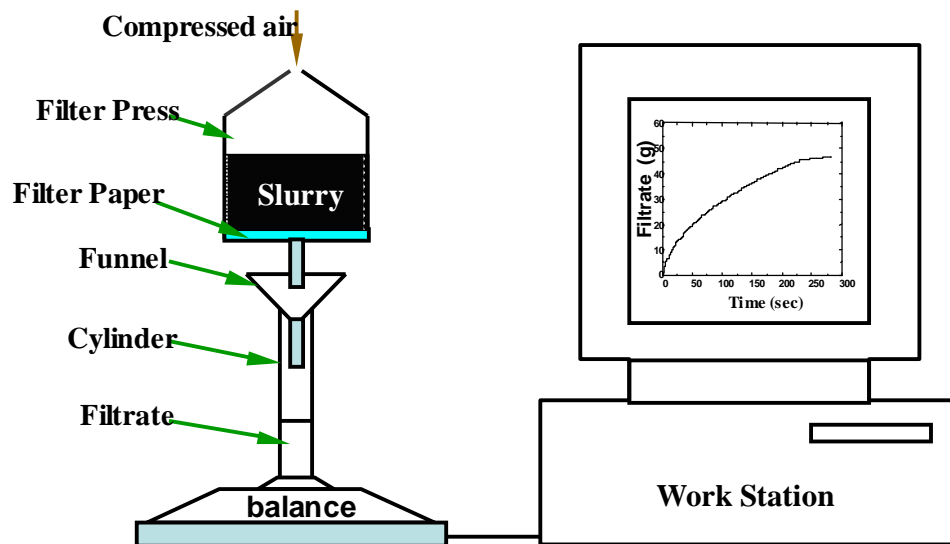


Figure 2. Illustration of the Filtration Setup

Filtration rate U can be determined from the slope of filtration curve. The filtration rate is mainly controlled by the cake permeability, which is greatly affected by particle size (Carman, 1948) when other process parameters are fixed.

The final moisture content of the cake, FMC, on the other hand, is determined by the total particle surface area and hydrophobicity. Filtration of coarse particles with more hydrophobic surfaces is in general more efficient, featuring higher U and lower FMC (Owen, 1985). Therefore, any technique that could increase particle size and surface hydrophobicity will improve filtration efficiency.

Filtration aids are often used to improve filtration efficiency in mineral processing. An ideal filtration aid should be able to modify the interfacial properties at the liquid-air and solid-liquid interface to effectively flocculate the particles and to increase their surface hydrophobicity (Yu, 1998). During the filtration process, the flocculated particles will facilitate the formation of filter cake with larger permeability resulting from the bigger porosity, leading to high filtration rate (Owen, 1985). The more hydrophobic solid surface, on the other hand, will result in lower final moisture content of the filter cake (Wheelock and Drzymala, 1991).

Many practical observations demonstrate that some commercial filtration aids are able to flocculate mineral particles and to enhance its surface hydrophobicity, leading to higher filtration efficiency (Geer, et al, 1959). In this study, many pre-selected promising filtration aids will be tested to achieve our research goals.

In most of the previous Cu/Ni concentrate filtration research, single filtration aid

could achieve both particle flocculation and surface property enhancement, and then led to high filtration efficiency. For the Cu/Ni concentrate used in this study, it turned out to be hard to find a single filtration aid that could improve both U and FMC. Many filtration aids tested could only improve either U or FMC.

The difficulty in finding a single filtration aid to improve filtration efficiency might result from the distinct properties, such as high pH and high Ca^{2+} concentration, of the concentrate used in this study. This difficulty may call for a different filtration strategy to improve the filtration efficiency. The fact that many single filtration aids could improve only U or FMC motivates us to have the idea that: if one filtration aid can achieve higher U and the other can achieve lower FMC, the combination of the two filtration aids may improve both U and FMC. This is one area where there has been little development to date to achieve desired filtration efficiency.

With this in mind, efforts in this study were made on three aspects: firstly, finding effective filtration aids that can minimize the FMC; secondly, searching for the filtration aids that can maximize U; and thirdly, trying the combination of the two filtration aids to improve both U and FMC.

The objective of this thesis is to investigate the suitability of filtration aids for

achieving highly efficient filtration for the Cu/Ni concentrate used in this study.

The fundamentals behind the filtration behavior are also investigated. The tasks under this study include:

- a) Conduct literature review to search for suitable filtration and dewatering theories and conduct experimental studies on filtration and dewatering enhanced by chemical additives.
- b) Following the conclusions reached by the previous Cu/Ni concentrate filtration research on the suitability of filtration aids, identify the surface charge characteristics of solid particles in the mineral concentrate, to assist the pre-selection of filtration aids suitable for effective solid aggregation and surface hydrophobicity enhancement.
- c) Based on the assumption that good settling performance is correlated with good filtration performance, perform bench scale settling tests to obtain instructive information for filtration tests. Although the assumption is found inaccurate, settling tests could provide useful guidance for filtration tests, and then filtration tests could be completed with much less effort.
- d) Investigate the surface charge characteristics of solid particles with the addition of different filtration aids to understand the role of surface charge in determining filtration aid performance.
- e) Determine particle size distributions of the concentrate with the addition of

different filtration aids, in order to establish a correlation between filtration performance and particle size, and to understand working mechanisms of the filtration aids.

- f) Investigate the effect of the addition of filtration aids on liquid viscosity and surface tension.
- g) Conduct filtration tests to evaluate the dewatering performance of each individual filtration aid in the context of both filtration rate and final moisture content. Based on the filtration performance, two filtration aids can be screened out: one is capable of lowering the final moisture content; and another is efficient in improving the filtration rate.
- h) Evaluate the filtration performance of the combination of two filtration aids to improve both filtration rate and final moisture content; explore the interaction effects between the two filtration aids
- i) Identify cake porosity and permeability with the addition of filtration aids.
- j) Investigate the effect of filtration aids on solid hydrophobicity, evaluating the correlation between solid surface hydrophobicity and final moisture content.
- k) Explore the working mechanism of filtration aids.

In this study, a series of tests with different filtration aids and their combinations are conducted to identify better filtration aids for higher filtration efficiency. After identifying the promising filtration aids, optimum filtration conditions are

determined. Zeta potential, particle size distribution, liquid viscosity, surface tension, cake porosity, cake permeability, and initial contact angle are determined to understand the working mechanism of filtration aids.

In chapter 1, the background of this thesis is introduced in a big picture. The theoretical framework, the general approach, the objective, and the main task of this thesis are also introduced. Chapter 2 provides literature review on the theories and practices of filtration and dewatering. Chapter 3 describes the details on the approach and supporting theories used in this thesis. Chapter 4 specifies the experimental set-up, materials, instrument and equipment used in this research, and describes the experimental procedure for completing this study. Chapter 5 presents the experimental results obtained by following the procedures specified in Chapter 4, and provides the scientific interpretations of the results. Based on the results and discussion, the working mechanism of the filtration aids is proposed. The conclusions and recommendations are given in Chapter 6 and Chapter 7, respectively.

CHAPTER 2. LITERATURE REVIEW

Vacuum filtration, as a conventional and economical filtration technique, is commonly used to dewater mineral slurry to certain moisture content, and then followed by thermal drying process to achieve the desired water removal (Owen, 1985). The development of highly efficient dewatering process will produce drier cake and reduce the load to thermal dryers, and then decrease the energy consumption used in the thermal drying process, resulting in the reduction of green house gas emissions (Singh, et al, 1998).

With respect to its nature, the approach of mineral slurry filtration research can be classified into two categories: purely theoretical approach and purely empirical approach. The purely theoretical approach deals with only mathematical expressions, contributing little to the solution of real industrial practices. The empirical approach provides practical solution to specific problems, but usually lacks generality for the specific filtration and dewatering practices. The combination of these two approaches might be an ideal methodology to provide practical solutions to the real industrial practices while maintaining certain level of generality.

This review focuses on two approaches. Firstly, an overall review of filtration and

dewatering theories will be presented. Secondly, the review of experimental studies of filtration and dewatering enhanced by chemical additives, including coagulant, surfactant, and flocculent (mainly polymer) will be provided.

2.1. Review of Filtration and Dewatering Theories

The water removal process of solid suspension by filtration could be divided into two distinct stages: filtration and dewatering.

2.1.1. Distinction between Filtration and Dewatering

A distinction is made between filtration and dewatering, asserting that filtration leads to the formation of cake whereas dewatering involves further cake moisture content reduction. During filtration stage, the bulk liquid from the slurry passes through the deposited solid cake and filter medium under mechanical driving force until all the liquid above the cake is removed. Only two phases, liquid and solid phases, are involved in filtration stage. The formed cake is assumed to be incompressible with constant structure. At the end of filtration stage, dewatering stage starts. Dewatering is described as a post-filtration process in which the liquid is displaced from the void space within the filter cake by the compressed air. Capillary effect and mass transfer regimes are significant for dewatering process. Three phases, liquid, solid, and gas, are involved during dewatering (Yu, 1998).

2.1.2. Filtration and Dewatering Theories

For research convenience, the water removal process is often modeled as filtrate being forced through a bundle of capillary channels within the cake. By the means of this model, many classical fluid mechanics theories and empirical equations can be applied to the analysis of water removal process. These classical theories, represented by mathematical equations, cannot evaluate and predict the filtration practice satisfactorily due to the complex nature of filter cake interacting with the liquid. However, these equations are useful for evaluating the effect of different parameters on the filtration performance.

A summary of the available filtration and dewatering theories proposed that Darcy's law, Brownell-Katz equation, and Laplace-Young equation are the three most useful equations to evaluate the filtration and dewatering practices. By combining Young-Laplace equation with the modified Darcy equation and Brownell-Katz equation, the effect of interfacial properties is incorporated in the filtration rate and moisture content equations (Owen, 1985).

Among the many controlling parameters involved in the above equations, surface tension (γ) and viscosity (η) of filtrate, affected by temperature and filtration aids added, are considered liquid related parameters; the remaining parameters –

cake permeability (k), contact angle (θ) and capillary radius (r) are important properties of solid impacting on filtration performance. The liquid and solid related parameters are practical to be manipulated for controlling the filtration efficiency. γ and η are strongly affected by temperature and filtration aids added. Lower γ and η contribute to efficient filtration. The parameters k and r are determined by cake structure, which is a strong function of particle sizes. Generally, filtration of coarse particle slurry will produce a cake with larger permeability and larger capillary radius. Particle aggregation often increases apparent particle sizes and hence pore radius, leading to larger cake permeability. Therefore, any factors affecting particle aggregation, such as particle surface charge or solid flocculation, will affect filtration performance through affecting k and r . Rendering the particles more hydrophobic, characterized by larger θ , on the other hand, will lead to lower final moisture content. Often particle aggregation is also enhanced by increasing hydrophobicity of particles, contributing to the enhanced k and r .

Filtration and dewatering practices proved that η was mainly controlled by temperature, not by the addition of filtration aids. The constant temperature maintained for most water removal process in the real industry suggests that η would be constant, and would not be a parameter practical to be altered for achieving efficient filtration. Therefore, above discussion clearly indicates that

cake permeability, surface tension, and solid hydrophobicity characterized by contact angle, are considered to be the three controlling parameters practical to be manipulated for efficient filtration.

2.2. Review of Filtration and Dewatering Practices

Chemical additives, including coagulants, surfactants and flocculants (mainly polymers), when used as filtration aids, can achieve an increased cake permeability, reduced liquid surface tension and enhanced solid hydrophobicity, resulting in better filtration performance.

2.2.1. Coagulants

Multivalent cationic coagulants, such as alum, iron, copper salts, lime, and inorganic acids, are widely used to enhance the filtration and dewatering of mineral slurry. It is believed that cationic metal ions would neutralize the negatively charged particle surface, reducing the electrostatic repulsive force to render the adhesion of solid particles. The adsorption of metal ions on solid surface might alter the surface hydrophobicity.

Some researchers studied the effect of alum salt on the filtration performance of

fine coal refuse. It was pointed out that the effectiveness of coagulant depends on the balance between attractive van der Waals forces and depressive force resulting from the electrical double layers of charged solid particles. Their results indicated that alum salt was effective in improving filtration rate but undesirably increased the final moisture content (Cheng, et al, 1988).

Other researchers also conducted research to investigate the effect of copper salts on the filtration performance (Khandrika, et al, 1994). They suggested that coal surface charge could be modified close to point of zero charge (PZC) through the addition of copper ions (using $\text{CuCl}_2 \cdot \text{H}_2\text{O}$). At PZC, electrostatic repulsive forces were minimized, facilitating the fine particle coagulation. The good coagulation produced a cake with high permeability that was desirable for the fine coal dewatering.

2.2.2. Surfactants

Knowledge of working mechanism of surfactants used in mineral slurry filtration is far from sufficient. The lack of understanding the working mechanism of surfactants leads to a wider divergence of views regarding the mechanisms of filtration enhanced by surfactants than those by other filtration aids, such as flocculants.

In contrast to the consideration that surfactants can only affect the surface tension of filtrate, a hypothesis is proposed that the effect of surfactants on filtration is achieved by affecting the three key dewatering parameters, that is, permeability, surface tension, and hydrophobicity (Owen, 1985). It suggested that, in addition to altering the surface tension by its adsorption of air-water interface, surfactants are also capable of adsorbing at coal-water interface. The adsorption of surfactant at coal-water interface might alter the solid surface hydrophobicity, and affect the state of flocculation of the particles.

Young-Laplace equation suggests that if surfactants were capable of lowering surface tension, it would reduce the capillary forces holding water in fine pores, and thus increase the effective filtration pressure, leading to a better filtration performance. To evaluate the validity of Young-Laplace equation, the filtration behavior of fine coal refuse was investigated by using an anionic (Aerosol –OT) and a nonionic (Triton X114) surfactant (Cheng, et al, 1988).

Some researchers explored the synergistic effects of flocculants, surfactants, and pH of the suspension in the single stage treatment to filter and dewater the ultra fine coal slurry (Singh, et al, 1998). Their research was based on the concept that the addition of flocculants changes the solid packing pattern and the separation distances in the particle matrix, which alters the permeability of the cake,

improving both the filtration rate and final moisture content. The role of surfactant addition is to lower the residual saturation of the cake by lowering the interfacial tension; and at certain pH, the minimization of electrostatic repulsive force will facilitate chemical additives to reach their best performance. In their research, cationic, anionic, and nonionic surfactants were used separately or in combination. The result demonstrated that significant improvement in final moisture content was obtained for all types of surfactants. The optimum filtration performance was achieved by using a flocculent followed by surfactant pretreatment.

2.2.3. Polymer Flocculants

The polymeric flocculants are the most important flocculants among all kinds. The application of synthetic polymer flocculants to coal dewatering goes back to the mid-1950s when such materials first became available (Yu, 1998). The capillary theory, represented by Young-Laplace equation, suggests that favorable flocculants are capable of reducing interfacial tension and viscosity, increasing the contact angle and capillary radius (namely, cake permeability), and finally leading to a decreased capillary pressure. Together with the increased cake permeability, both filtration rate and final moisture content will be improved by the addition of flocculants.

It was suggested that the basic working mechanism relevant to polymeric flocculants could be classified into two categories: the charge patch mechanism and the bridging mechanism (Owen, 1985). The former mechanism is mainly applied to the cationic polymer flocculation of the usually negatively charged particles by electrostatic attraction. The polymer molecule, relatively small in size as compared with the particles, covers only a small portion of the particle surface. However, its highly charged property effectively neutralizes a large area of the negatively charged solid surface. This cationic patch on one particle provides an attractive force to directly attach to the negatively charged sites on another particle, forming bigger agglomerates. When the bridging mechanism applies, the long polymer chain is adsorbed on particle surface only at a few points of attachment, leaving either ends or loops extending into the solution for contacting other particles.

Some researchers investigated the effect of polymeric flocculants on dewatering of fine coal refuse (Cheng, et al, 1988). They found that the addition of polymeric flocculants is the most effective way to improve the filtration performance. Their research also found out that the ionic nature, and polymer molecular weight, the dosage, the mixing time and mixing intensity play important roles in controlling the filtration performance.

Other researchers investigated the effect of FR-7A, a totally hydrophobic polymer, on the filtration of fine coal slurries by means of studying its adsorption behavior (Attia and Yu, 1991). Their research showed that FR-7A had a higher adsorption affinity to coal and pyrite than that to shale; an acidic slurry condition favored unselective adsorption of FR-7A on coal minerals, leading to improved total flocculation and filtration of fine coal slurry, while alkaline pH and the presence of SMP (sodium metaphosphate) favored selective adsorption and flocculation of coal from associated minerals in the slurry.

The use of polymeric flocculent in combination with coagulant or surfactant has also been explored in oil sands industry for improving settling fine solids. However, its application to filtration dewatering is rather limited in open literature.

CHAPTER 3. FUNDAMENTALS

A general filtration process can be viewed in two stages: filtration followed by dewatering, as shown in Figure 3.

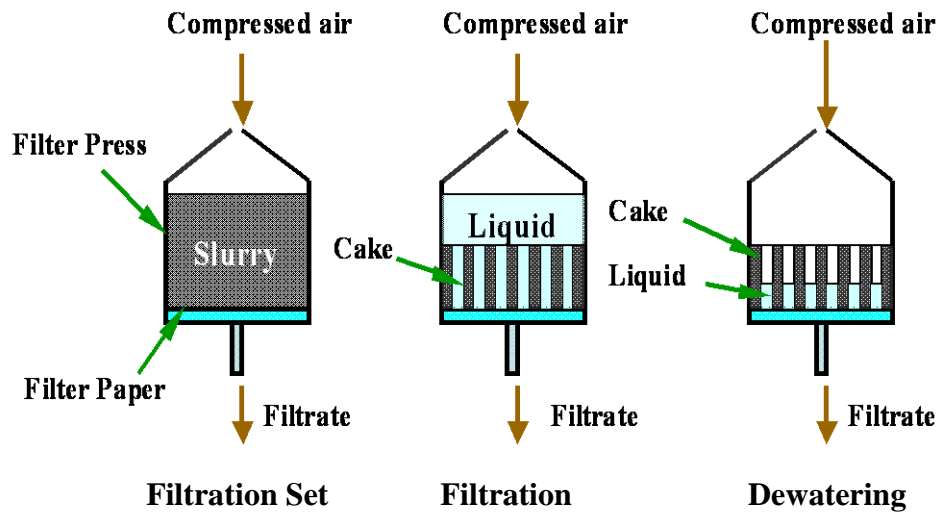


Figure 3. Schematic Illustration of a Filtration Process

During the filtration, the solids in the slurry settle down to form filter cake while the bulk liquid passes through the deposited solid cake under mechanical driving force, until all the liquid above the cake is removed (Yu, 1998).

Filtration stage can be subdivided into two phases: medium filtration and cake filtration. The first phase characterizes the process during which the slurry is mainly filtered by the filter medium until a full cake forms. In this stage, the

filtration curve deviates from straight line due to the increasing resistance as cake builds up. In the second phase, the remaining liquid above the cake is filtered through the full cake and medium, which is characterized by a straight line. During filtration stage, only two phases, liquid and solid phases, are involved. At the end of filtration stage, dewatering starts (Yu, 1998).

Dewatering is described as a post-filtration process in which the liquid is displaced from the void space within the filter cake under the application of the compressed air (Yu, 1998).

Dewatering stage can also be subdivided into two phases: capillary dewatering and mass transfer dewatering. Capillary dewatering is the phase during which the capillary effect is significant for the dewatering, it ends at the point when the last drop of bulk liquid is forced through the filter cake and air breaks through the whole cake. Following the capillary dewatering phase, the mass transfer dewatering phase starts to remove residual liquid in the cake. Three phases of liquid, solid and gas are involved during dewatering.

Figure 4 shows an example of various filtration stages with reference to filtration curve.

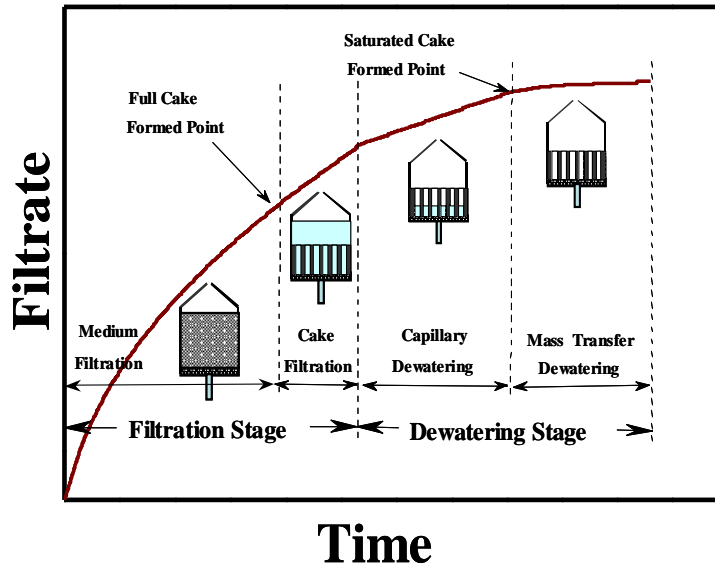


Figure 4. Distinction of Filtration Stages

Filtration stage, during which the liquid is forced through the porous filter cake, can be modeled as liquid passing through a bundle of capillary channels within the filter cake (Puttock, et al, 1986). By the means of this model, many classical fluid mechanics theories and empirical equations are applied to the analysis of water removal process. The fundamental equation describing the fluid flow through a capillary with circular cross section was derived by Poiseuille in 1840:

$$\frac{dV}{dt} = \frac{\Delta p \cdot \pi \cdot r^4}{8 \cdot \eta \cdot L} \quad (1)$$

where dV is volume of filtrates removed over a time interval of dt ,

Δp is the pressure drop across the capillary,

r is the radius of the capillary,

η is the dynamic viscosity of filtrate,

L is length of the capillary or thickness of the cake.

By means of Poiseuille equation, Darcy proposed the famous empirical Darcy equation in 1865 to describe liquid flowing through the porous filter cake. The modified Darcy equation is given by (Xu, et al, 1995):

$$U = \frac{1}{A} \frac{dV}{dt} = \frac{k \cdot (p - p_c)}{\eta \cdot L} \quad (2)$$

in which A is the filtration area,

k is the permeability of the cake,

p is the filtration pressure,

p_c is the capillary pressure,

Other parameters are the same as defined earlier.

In the modified Darcy equation (2), the left hand side term $\frac{1}{A} \frac{dV}{dt}$ is the linear velocity of filtrate passing through the cake. It characterizes the filtration rate (U).

Since $V = \frac{m}{\rho}$, the above equation can be rearranged to:

$$U = \frac{1}{\rho A} \frac{dm}{dt} = \frac{k \cdot (p - p_c)}{\eta \cdot L} \quad (3)$$

where m is the mass of filtrate, and ρ is the density of filtrate.

Based on the coal filtration experiment, Brownell and Katz in 1947 proposed an empirical equation of dewatering, relating the residual moisture content (S) of coal filter cake with cake structure parameter (k) and surface properties (γ and θ) as follows (Wheelock and Drzymala, 1991)

$$S = D \cdot \left[\frac{k \cdot (p - p_c)}{\gamma \cdot L \cdot \cos \theta} \right]^{-0.264} \quad (4)$$

where D is an empirical constant,

γ is the surface tension of the filtrate,

θ is the contact angle of the solid particle.

To describe the effect of interfacial properties on capillary pressure, Young and Laplace in 1982 proposed an equation in the form of (Morey, 2000):

$$p_c = \frac{2 \cdot \gamma \cdot \cos \theta}{r} \quad (5)$$

Combing Young-Laplace equation with the modified Darcy equation and Brownell-Katz equation, the effect of interfacial properties is incorporated in the filtration rate and moisture content equations.

From above equations, it is evident that U and S characterize the filtration rate and moisture content in the filter cake. Among the many controlling parameters, A , p and L are the mechanical factors determined by the given filtration facility subject

to equipment and economic considerations.

In the context of this study, the effect of filtration aids addition on the surface tension (γ) and viscosity (η) of filtrate can be considered negligible (see 5.6 and 5.7). The remaining parameters k , θ and r are the parameters practical to be manipulated to control the filtration efficiency.

The parameters k and r in the equations given above are determined by cake structure, which is a strong function of particle sizes (Attia and Yu, 1991). Concentrate of coarse particles will produce a cake with larger permeability and capillary radius. Particle aggregation often increases apparent particle sizes and then pore radius, leading to higher cake permeability. Therefore, any factors affecting particle aggregation, such as particle surface charge with filtration aid addition, will affect filtration performance through the change of k and r (Singh, et al, 1998). Rendering the particles more hydrophobic, characterized by larger θ , on the other hand, will lead to lower final moisture content in the filter cake (Attia and Yu, 1991). Often particle aggregation is also enhanced by increasing hydrophobicity of particles, contributing to the enhanced k and r (Xu, et al, 1995).

CHAPTER 4. EXPERIMENTS

4.1. Experimental Setup

The experimental setup is shown in Figure 2. The detail of the experimental procedure is described in Appendix 1.

An overview sketch of the experimental program employed in this study is given in Figure 5.

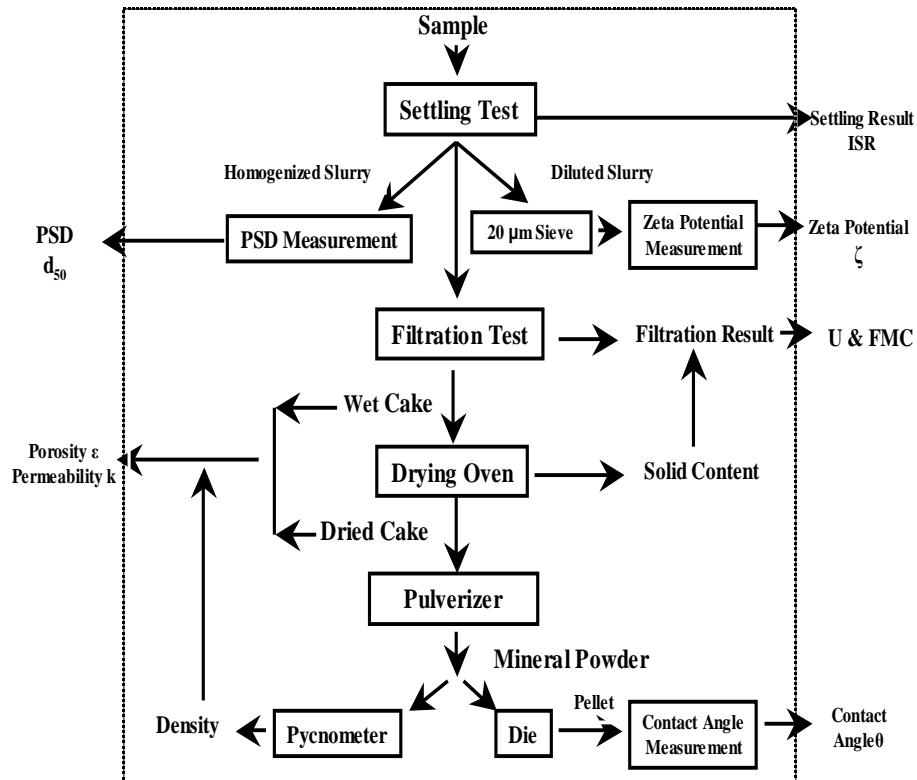


Figure 5. Overview of the Experimental Program

This program is characterized by the fact that one sample is used to conduct all the related tests. It minimizes the experimental error and sample inconsistency.

The prepared sample was first used to conduct the settling test to evaluate settling performance; ISR, initial settling rate, was obtained at this stage. After the completion of settling test, a tiny amount of the sample from the upper layer of the sediment with supernatant was taken out to conduct zeta potential measurement. The sample used for zeta potential measurement was returned to the original sample after zeta potential was obtained. After the original sample was fully homogenized, one or two drops of the slurry were taken out for particle size distribution measurement (characterized by d_{50}). The remaining sample was used to complete the filtration test to evaluate the filtration performance (U and FMC). After filtration, the wet cake was dried for getting solid content of the concentrate. The mass of wet and dry cake, as well as the thickness of wet cake, was recorded to get cake porosity and permeability when the solid density was measured. Thereafter, the dry cake was pulverized into solid powders that were screened to get fine particles. A small portion of the fine particles was used to measure the solid density, and the rest was put into a die to make pellet for initial contact angle measurement.

To characterize the rate of true filtration process, U is determined from the slope

of the cake filtration section of filtration curve in this study (see Figure 6). Although cake filtration process seems short during the whole filtration process, it reflects the structure of the filter cake. The slope of the cake filtration section is determined by the permeability of the cake (Khandrika, et al, 1994), which is also critical for the previous medium filtration phase and the following dewatering stage.

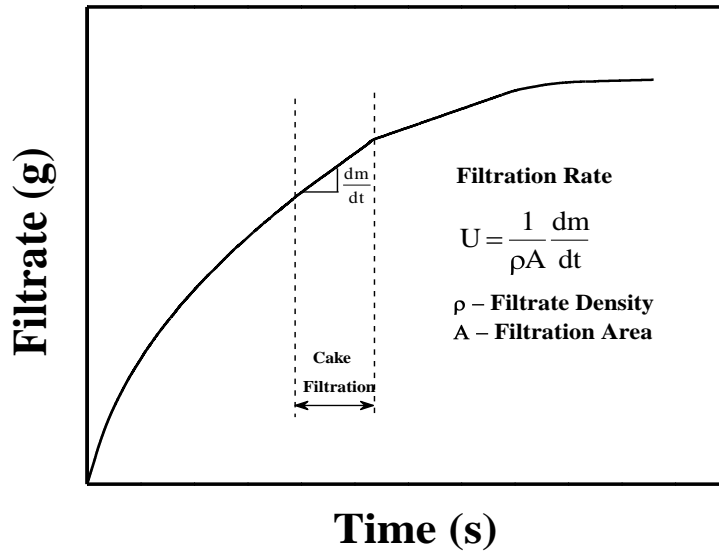


Figure 6. Determination of U

Using the following expression, the filtration result can be converted into the cake moisture content as a function of time.

$$MC(\%) = \frac{M \cdot (1 - sc) - M_f}{M - M_f} \cdot 100$$

where MC is the moisture content,

M is the mass of sample,

sc is the solid content of sample,

M_f is the mass of filtrate, which is a function of time.

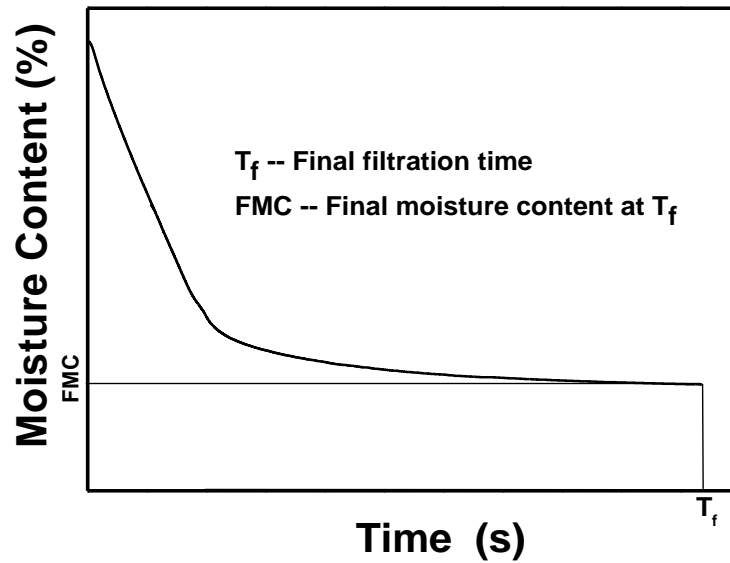


Figure 7. Determination of FMC

From this curve, the FMC – final moisture content, characterizing the moisture remaining in the cake at the end of given filtration time T_f , can be determined as shown in Figure 7.

Throughout this research, U and FMC are used to evaluate filtration performance.

A higher U and/or a lower FMC characterize a better filtration performance.

4.2. Experimental Materials

Vale-Inco Metals Ltd. provided Cu/Ni concentrate. The composition of the bulk concentrate is given in Table 1. The supernatant composition analyzed by atomic absorption spectrophotometer (AAS) is presented in Table 2.

Table 1. Sample Composition (Wt % on Dry Basis, pH = 12)

Chalcopyrite (CuFeS ₂)	Pentlandite ((FeNi) ₉ S ₈)	Pyrrhotite (Fe _{n-1} S _n)	Cobalt (Co)	Silicon (Si)	Silica (SiO ₂)	Ca
5~10	15~40	30~60	0.1~1	1~5	1~3	1.73

Table 2. Composition (AAS) of Supernatant (ppm)

Ca ²⁺	Fe ^{x+}	Co ²⁺	Cr ²⁺	Cu ²⁺	Ni ²⁺
48.8	< 0.05	< 0.05	0.08	0.28	0.06

The composition of the Cu/Ni concentrate used in this study indicates that, comparing with the normal Cu/Ni concentrate from mineral processing industry, a significant portion of copper sulfides (Chalcopyrite) is removed, and the pH and Ca²⁺ concentration are extremely high. These distinctive characteristics may require different dewatering strategies to achieve efficient filtration.

As a critical parameter for mineral processing, pH affects the filtration behavior

through two different ways. Firstly, the function of some filtration aids is greatly affected by concentrate pH. For example, some filtration aids, such as A100, will decompose quickly at high pH condition (i.e. ~12). Secondly, as a potential determining factor, pH affects the surface charge properties of the solid particles. For specific mineral concentrate, the pH at which the surface potential is zero is called iso-electronic point (iep). At iep, solid particles tend to coagulate easily to form bigger agglomerates with altered surface properties, affecting the U and FMC.

The high concentration of Ca^{2+} in the concentrate greatly affected the dewatering strategy. Many previous filtration tests for Cu/Ni concentrate confirmed that anionic filtration aids were suitable for achieving good filtration performance. Given the negatively charged solid surface, it seems reasonable for cationic filtration aids to be effective to adsorb onto solid surface and improve filtration efficiency. The strange observation might result from the effect of Ca^{2+} contained in the concentrate. Although the solid surface was negatively charged, some Ca^{2+} ions adsorbed onto the solid surface resulted in strong positively charged patches on the solid surface. These positive patches attracted anionic filtration aids to adsorb onto the solid surface to work as coagulant affecting filtration performance.

The filtration aids tested in this study are given in Table 3.

Table 3. Filtration Aids Used in This Study

Name	Code	Type	Source
Aerodri 100	A100	Anionic surfactant	Cytec
MagnaFloc 1011	MF	Anionic polymer	Ciba
Dodecylamine Hydrochloride	DAH	Cationic surfactant	Acros

MF stock solution was prepared in 500 ppm concentration by 48 hours low speed shaking, A100 and DAH stock solution was diluted to 1 wt % by 20 minutes low speed shaking.

4.3. Instrument and Equipment

As shown in Figure 2, the experimental setup consists of a filter press (Series 300 API, Fann), compressed air cylinder, an electronic balance, and a computer data acquisition system. Filter paper used in this study is 3.5 inch in diameter from Osprey Scientific Inc.

A lab stirrer (RZR2000, Caframo) was used to prepare the sample. ZetaPals (BrookHaven), Mastersizer 300 (Malvern) and Drop Shape Analysis (DSA10,

Krüss) were used to measure zeta potential, particle size distribution, and initial contact angle, respectively.

A lab pulverizer and a set of die (1”) were used to make pellet from dry mineral powder. A 25 ml pycnometer was used to determine the solid density that is used to calculate the porosity of the saturated cake.

4.4. Filtration Test Procedure

See Appendix 1 for the detailed information on filtration test procedures.

Table 4 lists the major experimental conditions for this research.

Table 4. Experimental Conditions

Pressure (Pa)	Sample size (g)	Filtration duration (s)	pH	Solid content (wt %)
1.034x10⁵	~100	150	11.3~11.5	62.5

4.5. Experimental Procedure

The major measurements in this project were settling and filtration performance.

To understand the mechanism responsible for filtration characteristics, zeta potential, particle size distribution, liquid viscosity, surface tension, cake porosity,

cake permeability, and initial contact angle were investigated. The pH of the slurry was recorded whenever applicable.

4.5.1. Surface Charge of Original Concentrate

The surface charge of solid particles in the original concentrate is evaluated by zeta potential. For zeta potential measurement, the sample preparation is important. The preparation of suspension having a defined dispersion state – which does not change during measurement – is possibly the most important prerequisite.

Due to the high solid content and wide range of solid particle size distribution, the mineral concentrate was first diluted and screened before measurement. The dilution of the concentrate was achieved by first re-suspending a few drops of fresh concentrate into the supernatant mother liquor, and then screening the diluted slurry using a 20 μm sieve. In this way the chemical environment of the original sample was maintained while reducing the solid content and size to the desired level: 0.05 ~ 0.1 wt% and 5 nm ~ 30 μm . With this procedure, the pH and other properties of the diluted slurry sample would also be kept the same as the samples used for the filtration tests.

4.5.2. Correlation between Settling and Filtration Performance

If tests were directly started with filtration, the whole process would be very time, energy, and sample consuming. A more efficient way is to conduct a few screening tests to obtain some instructive information for filtration test. Settling test was chosen as the screening test in this study. For example, if the slurry positively responded to filtration aid in settling, it was very likely that this filtration aid would facilitate filtration. Following the information obtained, the evaluation of filtration performance could be completed with much less effort. During settling tests, the volume of the settled sediment, more specifically the mud-line, was recorded as a function of time. The volume reading, equivalent to the height of the mud-line, at a certain time, reflected the settling efficiency. A lower volume indicated a higher settling efficiency.

The reason for choosing settling as the screening test results from an assumption that settling performance is correlated with filtration performance. This assumption suggests that, for a specific filtration aid, quick settling corresponds to a good flocculation of solids and then corresponding to a good filtration performance. If the solid could be made more hydrophobic, the FMC would be low. The sample preparing procedure for settling test is the same as that for filtration test, as described in Appendix 1.2, except that the prepared sample

should be diluted to 40% using the original supernatant. Settling performance was evaluated by the initial settling rate (ISR). The determination of ISR is illustrated in Figure 8.

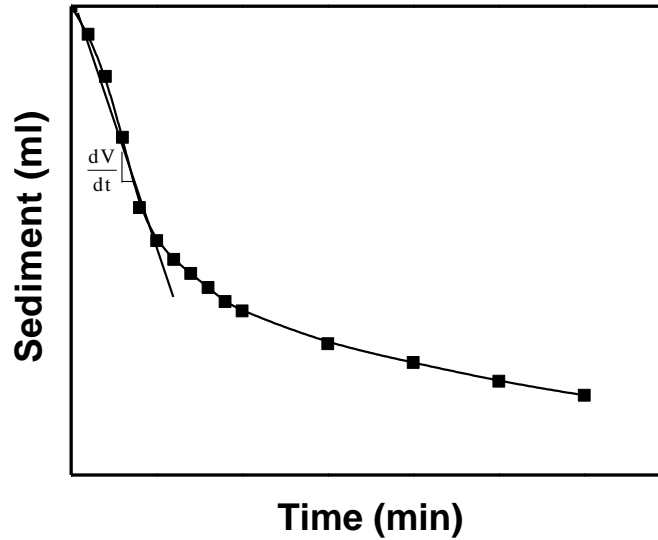


Figure 8. Determination of ISR

The ISR is calculated from experimental values $\frac{dV}{dt}$ using expression

$$ISR = - 3.04 \times 10^{-5} \times \frac{dV}{dt} \text{ (m/s)}$$

The “-” sign is used to convert negative $\frac{dV}{dt}$ value into positive, 3.04×10^{-5} is used to convert volume scale into length scale by using the geometric parameters of the cylinder used for settling tests (100 mL equivalent to 0.182 m).

4.5.3. Filtration Test

At the beginning of this study, great efforts were made by using single filtration aid to achieve both high U and low FMC. Although this objective was not achieved, some filtration aids were found effective in achieving either high U or low FMC. Based on their performance, filtration aids were categorized into two types: the first type like A100 could achieve lower FMC, the second type like MF could achieve higher U. The combination of the two types of filtration aids was tested. The order of the addition of two filtration aids was also tested for further improving filtration performance.

In the case of finding optimum dosage of single filtration aids, the filtration process before the mass transfer dewatering phase (see Figure 4) was sufficient to evaluate the effect of filtration aids. Therefore, U and SMC – saturated moisture content of the cake were used to evaluate the filtration performance. The higher U means a quicker filtration; the lower SMC indicates more hydrophobic solid. SMC and FMC were equivalent for evaluating the effect of solid hydrophobicity.

Based on the definition of saturation, the saturation of cake was reached when the last drop of bulk water was drained out of the cake. In the test, the saturation point was marked by the first air bubble coming out of the filter press.

To evaluate filtration performance sufficiently, the whole filtration process including mass transfer dewatering was needed. In this case, U and FMC – final moisture content of the final cake were used.

In this study, the sample from settling tests was used for filtration tests.

4.5.4. Process Optimization

The filtration performance of A100 + MF at each individual optimum dosages might not be at the optimum when combined together. The interaction effects between A100 and MF might occur and the optimum performance might locate at other dosage combinations. The interaction effect between the two filtration aids should be investigated for further improving filtration performance of A100 + MF combination. This exploration is to achieve process optimization.

To search for the optimum filtration performance of A100 + MF, two attempts were made during this study. One attempt was made to change the dosage of A100 only and keep the dosage of MF at its individual optimum dosage. Another attempt was made by keeping A100 at its individual optimum dosage and changing the dosage of MF. Through these attempts, the optimum performance of A100 + MF might be located.

4.5.5. Sample Zeta Potential Measurement

The procedure for sample zeta potential measurement was the same as that described in 4.5.1.

The sample used for zeta potential measurement was prepared from the sample used for settling tests. Upon the completion of settling tests, a tiny amount of solids from the upper layer of the sediment was taken out and screened by a 20 μm sieve. The solid passing through the sieve was diluted by using the supernatant of settling test. In this way the sample used for zeta potential measurement was the same as that used for settling tests and filtration tests.

4.5.6. Particle Size Distribution Measurement

In order to verify the effect of filtration aids on particle aggregation, particle size distribution was measured using Malvern Mastersizer 300. It should be noted that the particle size distribution determined as such was only used as an indicator of particle aggregation as the aggregates formed may break during the particle size measurement by mixing.

The sample was taken from the settling test after fully homogenized by shaking.

The Mastersizer was set at 3,000 rpm when measuring.

4.5.7. Effects of the Addition of Filtration Aids on Filtrate Viscosity

Conventionally, the fully formed cake during filtration can be considered incompressible. Based on this assumption, we can define a constant $C = \frac{\rho \cdot A \cdot k \cdot p}{L}$ as such that the modified Darcy equation in Chapter 3 could be arranged to the following form

$$\frac{dm}{dt} = \frac{C}{\eta} \quad (6)$$

This expression indicates that the filtration rate U is inversely proportional to the liquid viscosity (η).

For the filtration aids added to the slurry, if not all of them are adsorbed onto the solid surface, some filtration aids would remain in the liquid and might change its viscosity. Due to the significant effect of liquid viscosity on filtration performance (Wakeman, 1977), tests were conducted to verify whether the viscosity change due to the addition of filtration aids is significant in this research.

To evaluate the viscosity of filtrate by using expression 6, filtration tests were performed by refilling 41.5 g filtrate of the 350 g/t A100 filtration test and 41.5 g

supernatant of blank concentrate into the filter press with the same saturated filter cake formed from 350 g/t A100 sample. In this way, the identical filtration conditions were ensured.

Based on expression 6, the slope of cake filtration part of the filtrate curve would provide the information of liquid viscosity. The linear filtration curve indicated a constant viscosity during the filtration process, while the same slope of filtration curves indicated the same viscosity of the two refilled liquids. If the two curves were both linear with identical slopes, the effect of filtration aids addition on viscosity would be insignificant for filtration, and the viscosity change caused by filtration aids addition was negligible.

4.5.8. Effects of the Addition of Filtration Aids on Surface Tension

Filtration aids that are not adsorbed onto the solid surface would remain in the liquid and might change the surface tension of liquid. Due to the significant effect of surface tension on capillary pressure, and then filtration performance (Wakeman, 1977), tests were conducted to verify whether the surface tension change caused by filtration aid addition was significant for filtration performance. In this test, the filtration curve corresponding to capillary dewatering was used to conduct the evaluation.

Substituting Young-Laplace equation into the modified Darcy equation in Chapter 3, the following expression could be obtained:

$$\frac{1}{\rho A} \frac{dm}{dt} = \frac{k_s \cdot \left(p - \frac{2 \cdot \gamma \cdot \cos \theta}{r} \right)}{\eta \cdot L}$$

Rearranging this expression leads to:

$$\gamma = \frac{r \cdot p}{2 \cos \theta} - \frac{r \cdot \eta \cdot L}{2 \rho \cdot A \cdot k_s \cdot \cos \theta} \frac{dm}{dt}$$

For a given saturated cake, capillary radius (r), contact angle (θ), cake thickness (L), and saturated permeability (k_s) are all constants. Other parameters - filtration pressure (p), filtration area (A), and density (ρ) are also constants. If viscosity (η) were proven constant in 4.5.7, the identical constant $\frac{dm}{dt}$ for the two liquids would indicate a negligible effect of filtration aids on surface tension.

4.5.9. Saturated Cake Porosity and Permeability Measurement

Saturated cake porosity (ε) was defined as the ratio of void volume filled by liquid to total volume of the saturated cake. This definition results in an expression:

$$\varepsilon = \frac{\rho_s \cdot (m-1)}{\rho_1 + \rho_s \cdot (m-1)}$$

where $m = \frac{w_{sc}}{w_s}$

ρ_s is the density of the solid,

ρ_1 is the density of the liquid,

w_{sc} is the saturated cake weight,

w_s is the weight of dry solids in the saturated cake.

For a cake to reach saturation under a given pressure, the compressed air provided driving force to push the liquid out of the voids, penetrating through the cake. The void within the saturated cake was not fully filled by liquid; rather it was partially filled by air. In this study, the cake was modeled as a bundle of capillary tubes. This model suggested that all the extra liquid mainly occupied the capillary tubes, i.e. this was the only liquid removed from cake to reach the saturation. The remaining part of the cake was always kept at saturation. After all the extra liquid was removed from the capillary tubes, saturated cake was produced. All the air within the cake stayed in the tube. After completion, the compressed air was removed; the air in the cake would be forced out. Actually, there was no tube in the cake. From this view, saturated and incompressible cake assumption was reasonable.

Saturated cake permeability (k_s) was obtained from the filtration result.

Rearranging the modified Darcy Equation into the form:

$$k_s = \frac{\eta \cdot L}{\rho \cdot A \cdot (p - p_c)_s} \frac{dm}{dt}$$

where $(p - p_c)_s$ is the pressure difference across the saturated cake.

The cake from filtration test was used to measure the saturated porosity and permeability. The wet cake was dried in a drying oven after filtration test.

4.5.10. Initial Contact Angle Measurement

Contact angle (θ) of the solid measured the hydrophobicity of solid surfaces. To determine the effect of filtration aids addition on solid hydrophobicity, the dried solid from the filtration cake was compressed into pellets for the initial contact angle measurement. The dried cake from the filtration test was first pulverized into powder that was then screened by a 53 μ m sieve, and then the -53 μ m powder was compressed into pellet in a 1 inch die under 0.38 MPa for 4 minutes.

During initial contact angle measurement, a water drop was generated to contact the top surface of the pellet. Due to the porous structure of the pellet, the water drop penetrated into the pellet continuously and a stable contact angle could not be obtained. For this reason, the initial contact angle, upon the contact of water drop with the pellet, was measured.

4.5.11. Backwashing with Surfactants

To be effective in filtration, filtration aids should adsorb onto the solid surface at first, and then flocculate the solid and alter solid hydrophobicity. The adsorption of filtration aids onto solid particles requires a close contact between filtration aids and solid surface. For the normal filtration test, sample is prepared by mixing filtration aids with slurry. The water contained in the slurry might disturb the adsorption of filtration aids onto solid surface. If the free water in the slurry were removed, the solid surface would be directly exposed to the filtration aid added, resulting in more effective adsorption than the case of addition in the slurry.

With this in mind, the sample slurry was filtrated at first to remove the free water. At the end of the capillary dewatering phase, all the bulk liquid was removed from the cake and the compressed air started to blow through the cake. This time point is called breakthrough point (i.e, saturated cake formed point in Figure 4). It is characterized by the first air bubble coming out of the spout of the filter press. The filtration was stopped when reaching the breakthrough point. One third of the filtrate was taken out of the cylinder to make the surfactant solution. The surfactant solution was then refilled into the filter press. After the filter press was left still for 5 minutes, the filtration was restarted.

Due to the negative charge of the solid surface, cationic surfactant seems easier to adsorb onto the particle surface. The cationic surfactant solution used for cake backwashing was 7.5 g/t DAH based on the basic sample for filtration with 350 g/t A100 + 5.5 g/t MF addition.

CHAPTER 5. RESULTS AND DISCUSSION

The experiments described in Chapter 4 produced the following results. The significance of the result is discussed in this chapter.

5.1. Surface Charge of Original Concentrate

The surface charge of solids in the original concentrate was negative. Unfortunately, the measured surface charge (i.e. zeta potential) was inconsistent from test to test. The inconsistency, typical for sulfide suspensions, indicated a complex surface charge property. The zeta potential values (ζ) measured are given in Figure 9. The detailed raw data are given in Table A2.1 in Appendix 2.

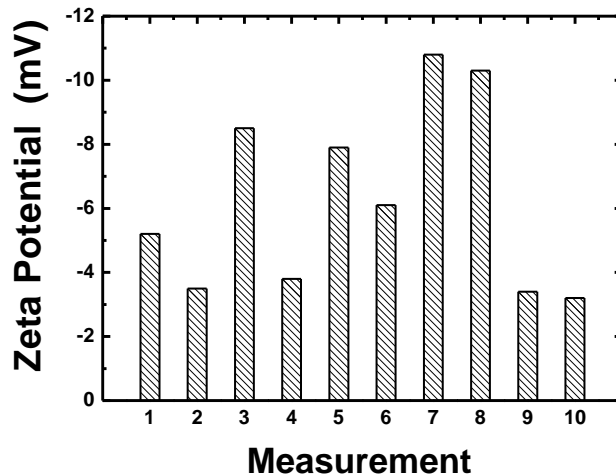


Figure 9. Zeta Potential of Original Concentrate

Overall, the measured zeta potential values were relatively small. The weak zeta potential might result from the high ionic strength of the concentrate, which significantly compressed electrostatic double layers. During the upstream beneficiation process, many chemical additives were added into the slurry to facilitate the formation of concentrate. These chemicals along with ions released from minerals might contribute to the compression of electrostatic double layers.

5.2. Correlation between Settling and Filtration Performance

5.2.1. A100

The result of settling tests with A100 addition is presented in Figure 10, the correlation between settling and filtration performance is presented in Figure 11 - 12. (See Table A2.2 and Table A2.4 in Appendix 2 for detailed data).

Figure 10 illustrates the settling performance of A100 at different dosage with the blank as basis. The ISR of A100 at different dosage is obtained from the settling results. The result shows that the addition of A100 improves the settling performance, resulting in smaller volume of sediment at a given time comparing with that of blank. ISR increases with increasing A100 dosage until the dosage reaches 350 g/t. After that further increase of dosage decreases ISR. Through this

set of tests, the optimum ISR was found at the dosage of 350 g/t.

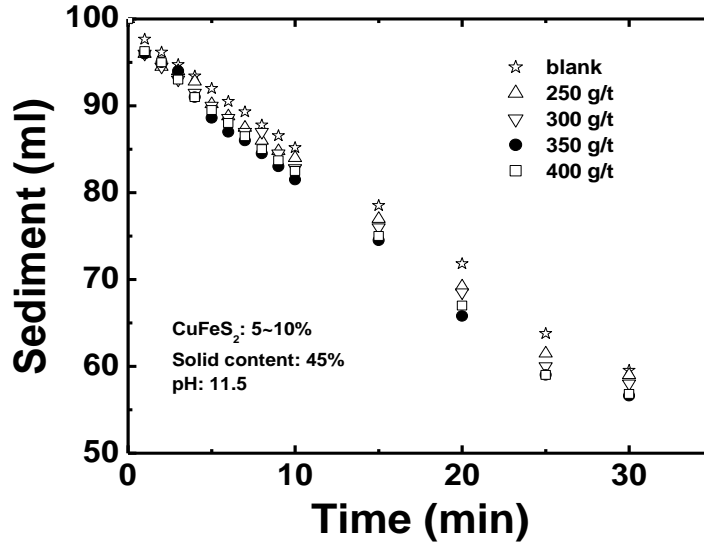


Figure 10. Effects of A100 Addition on Settling Performance

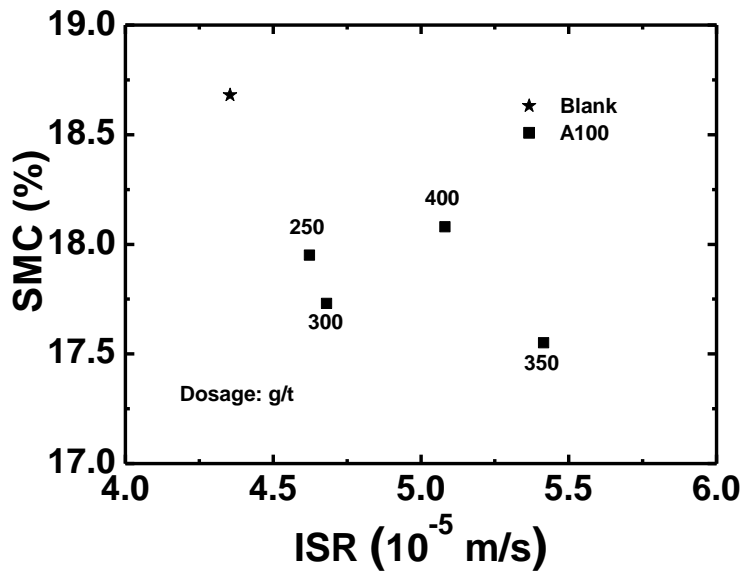


Figure 11. ISR - U with A100 Addition

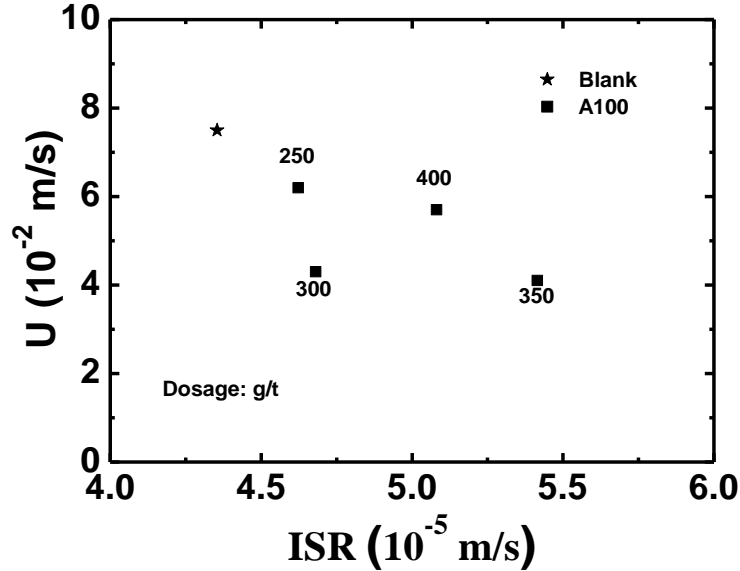


Figure 12. ISR - SMC with A100 Addition

Upon the completion of settling tests, the sample was used to do the filtration tests. Filtration rate (U) and saturated moisture content (SMC) were obtained from the filtration curves. The related filtration curves are given in Figure A3.1 and Figure A3.2 in Appendix 3.

Figure 11 correlates ISR with U and Figure 12 correlates ISR with SMC. In general, U and SMC decrease with increasing ISR. The results suggest that, with the addition of A100, higher ISR correlates with lower U and lower SMC.

This finding partially contradicts with the assumption that good settling performance (high ISR) correlates with good filtration performance (high U and

low SMC). The filtration results suggest that A100 disperses the slurry, decreasing the filtration rate, however, it makes particle surfaces more hydrophobic. Based on the benefit of reducing SMC, an optimum dosage is suggested at 350 g/t.

5.2.2. MF

Figure 13 presents the result of settling tests with MF addition. (See Table A2.2 in Appendix 2 for detailed data).

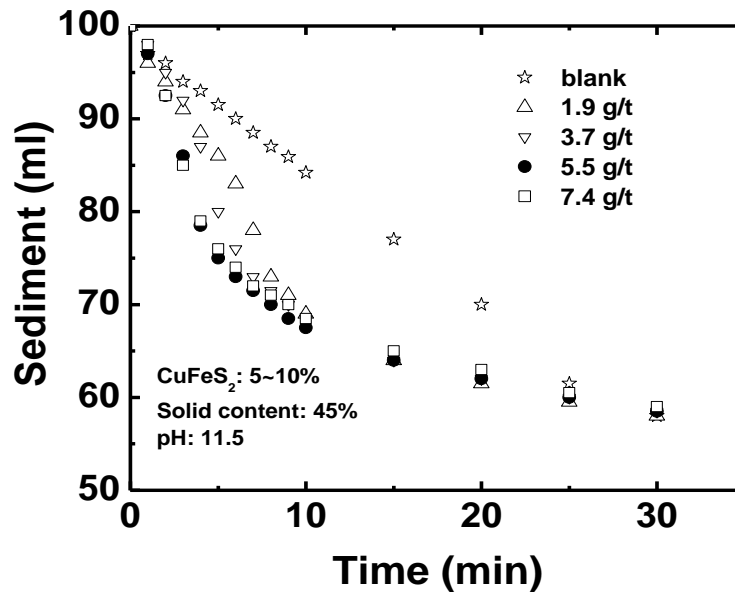


Figure 13. Effects of MF Addition on Settling Performance

The result suggests that the addition of MF greatly improved the settling performance, indicating formation of large aggregates. The results show that the ISR increased with increasing MF dosage until MF dosage reaches 5.5 g/t, where

additional MF showed marginal impact on further ISR increase. Optimum ISR is found at the dosage of 5.5 g/t.

From the filtration curves given in Figure A3.3 - A3.4 in Appendix 3, the U and SMC values are obtained (See Table A2.4 in Appendix 2 for detailed data). Figure 14 correlates ISR with U and Figure 15 correlates ISR with SMC. In contrast to the results obtained with A100 addition presented in 5.2.1, U increases with increasing ISR while SMC seems insensitive to MF addition. The results are anticipated as flocculation of solid particles by MF increases capillary radius within the cake for effective filtration. The hydrophilic nature of MF does not improve solid hydrophobicity, leading to none improvement in SMC.

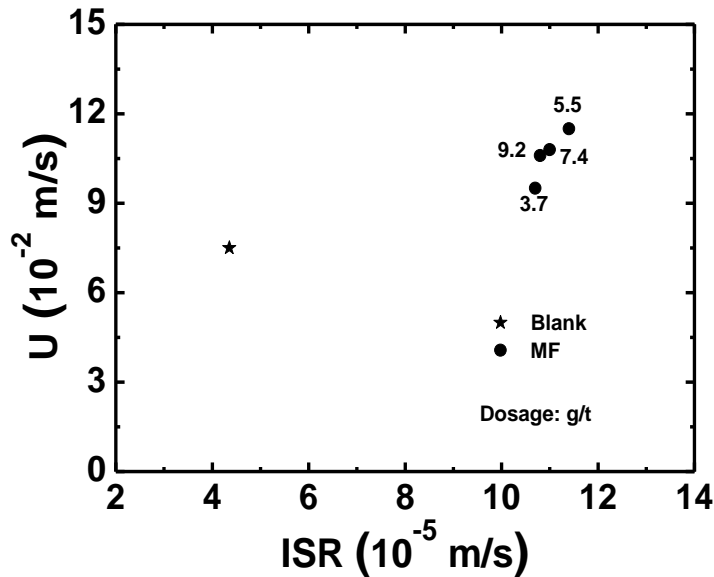


Figure 14. ISR - U with MF Addition

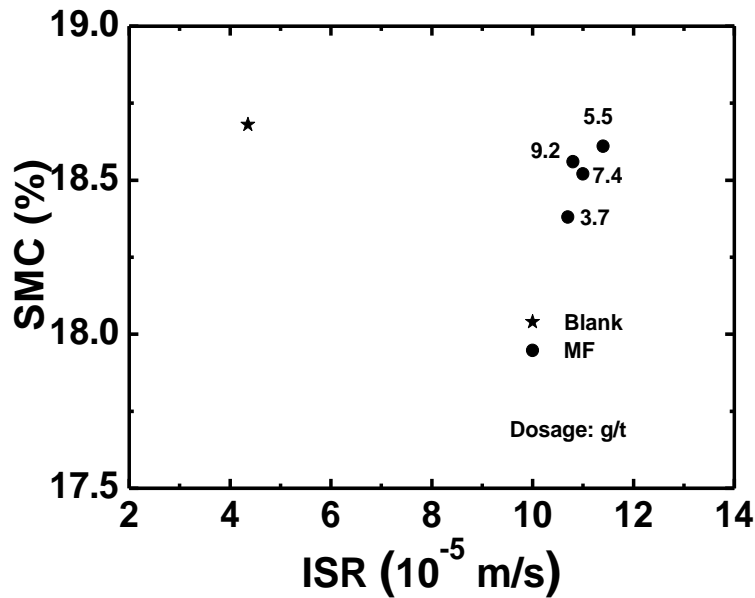


Figure 15. ISR - SMC with MF Addition

An optimum dosage of 5.5 g/t is identified to produce the highest ISR and U

5.2.3. A100 and MF

Based on the results in 5.2.1 and 5.2.2, at their optimum dosage, 350 g/t A100 produced the lowest SMC; 5.5 g/t MF produced the highest U. It is easy to expect that the combination of 350 g/t A100 and 5.5 g/t MF might produce both highest U and lowest SMC. Figure 16 presents the result of settling tests with A100 and MF addition (The detailed data are given in Table A2.2 in Appendix 2).

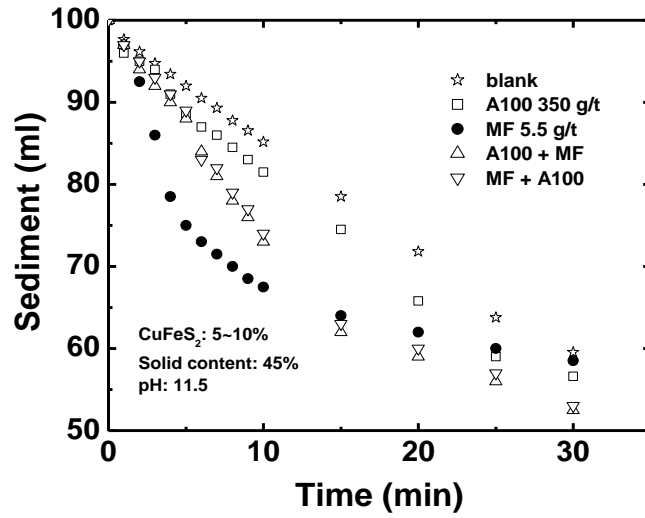


Figure 16. Effects of A100 and MF Addition on Settling Performance

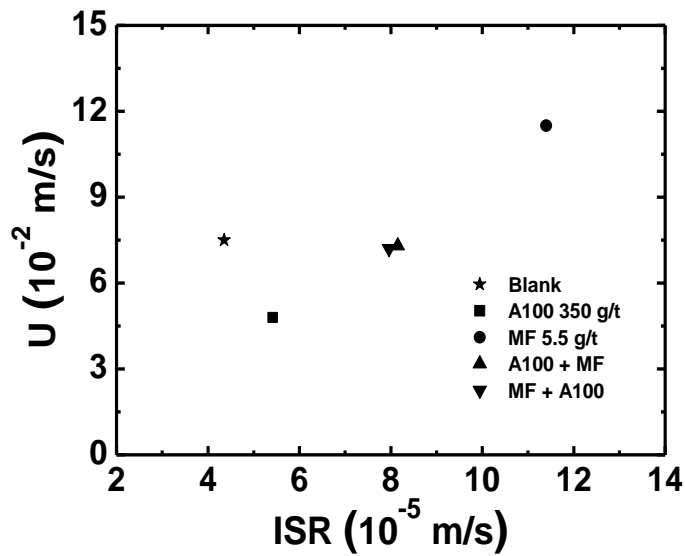


Figure 17. ISR - U with A100 and MF Addition

Figure 16 shows that MF achieves the highest ISR, A100 achieves the lowest ISR, while A100 + MF and MF + A100 present similar ISR between the two extremes.

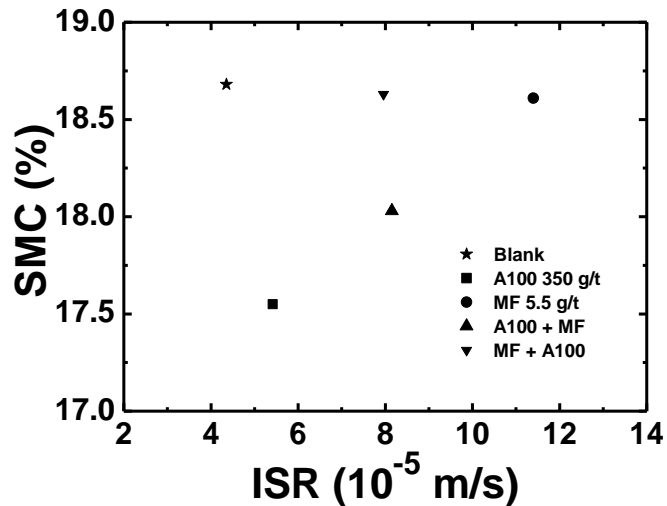


Figure 18. ISR - SMC with A100 and MF Addition

From the filtration curves given in Figure A3.5 and Figure A3.6 in Appendix 3, the U and SMC values are obtained (See Table A2.4 in Appendix 2 for detailed data). Figure 17 correlates ISR with U and Figure 18 correlates ISR with SMC. The results in Figure 17 show that, even though MF could increase ISR and U significantly, the presence of A100 depressed the flocculation of solid particles by MF addition, leading to lower value of ISR and U. The order of addition of MF and A100 did not show significant effect on both ISR and U.

Figure 18 shows no clear correlation between ISR with SMC. However, A100

addition could reduce SMC, even if MF was present, although to a less extent as compared with A100 alone. The order of A100 and MF addition showed a significant impact on SMC values: the combination of A100 + MF produced lower SMC than the combination of MF + A100.

The above settling and filtration test results suggest that higher ISR does not necessarily correspond to better filtration performance evaluated by U and SMC. The order of A100 and MF addition is significant for SMC, but insignificant for U.

5.3. Process Optimization

To evaluate the saturated cake structure, filtration tests above were terminated when the cake reached its saturation. SMC rather than FMC was obtained from the test. Some tests with A100 and MF producing SMC only were repeated to evaluate its whole filtration process performance with FMC produced. Their SMCs and FMCs are plotted in Figure 19 (Related data see Table A2.4 – Table A2.5 in Appendix 2).

Figure 19 shows that SMCs and FMCs present a linear relation with a slope close to 1. This correlation indicates that FMC and SMC are equivalent to evaluate the

same property - hydrophobicity. Therefore, in the following sections of this thesis, FMC, rather than SMC, is used to evaluate solid particle surface hydrophobicity.

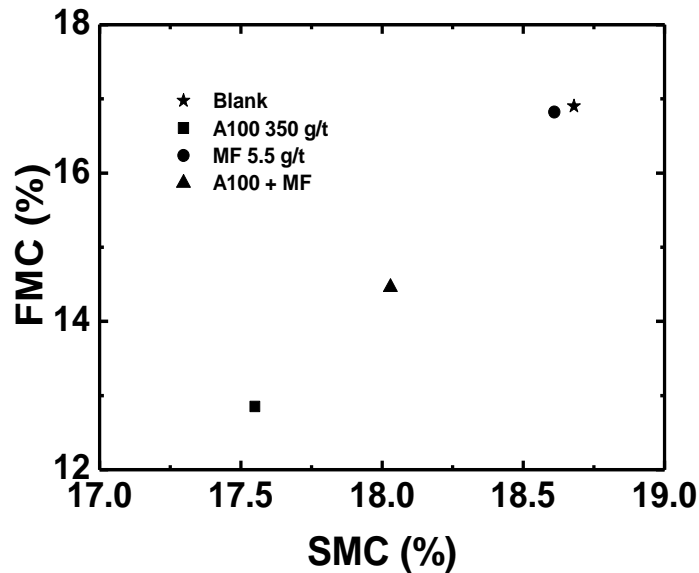


Figure 19. SMC – FMC with A100 and MF Addition

The result of 5.2.3 indicated that 350 g/t A100 + 5.5 g/t MF improved filtration efficiency only to a certain degree, the filtration performance of A100 + MF at each individual optimum dosages might not be at the optimum when combined together, as described in 4.5.4.

To search for the optimum filtration performance of A100 + MF, one attempt was made to change the dosage of A100 and keep the dosage of MF at 5.5 g/t in the combination of A100 + MF. Another attempt was made by keeping A100 at 350

g/t and changing the MF dosage for A100 + MF. Figure 20 illustrates the results of FMC - U obtained at x g/t A100 + 5.5 g/t MF and 350 g/t A100 + y g/t MF. The filtration curve of x g/t A100 + 5.5 g/t MF is shown in Figure A3.7 and Figure A3.8 in Appendix 3; the filtration curve of 350 g/t A100 + y g/t MF is shown in Figure A3.9 and Figure A3.10 in Appendix 3; detailed data are given in Table A2.5 in Appendix 2.

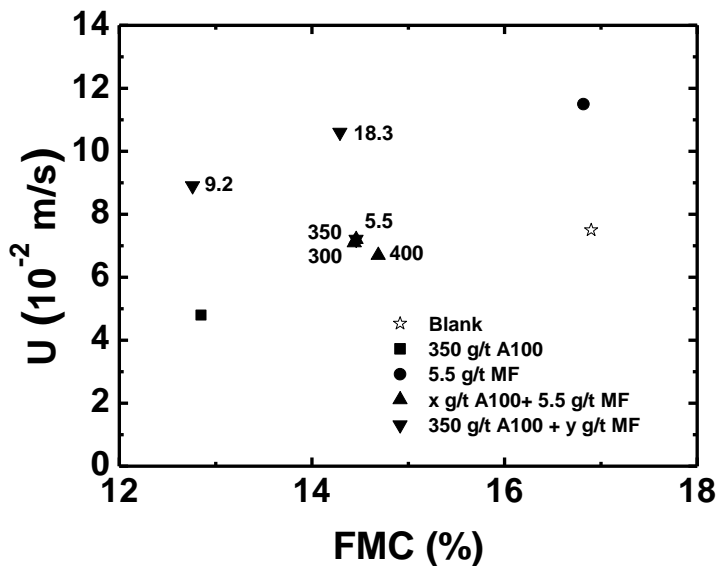


Figure 20. FMC - U with x g/t A100 + y g/t MF Addition

It is evident that changing A100 dosage at 5.5 g/t MF has little effect on U and FMC. This finding indicates that changing A100 dosage in this combination is not an effective way to improve filtration performance.

Figure 20 also shows the U and FMC of 350 g/t A100 + y g/t MF. The result suggests that changing MF dosage in the combination of A100 + MF may be an effective way to locate the optimum dosage.

The result shows that the filtration performance of 350 g/t A100 + 9.2 g/t MF and 350 g/t A100 + 18.3 g/t MF is much better (closer to up-left corner of the figure) than that of 350 g/t A100 + 5.5 g/t MF. Although 350 g/t A100 + 18.3 g/t MF produces a higher U than that of 350 g/t A100 + 9.2 g/t MF, but its FMC is higher. If the preference was given to U, 350 g/t A100 + 18.3 g/t MF would be a better choice. If FMC was preferred, 350 g/t A100 + 9.2 g/t MF would be a better choice. Considering the larger MF consumption in the former and reducing FMC is the target for industry, 350 g/t A100 + 9.2 g/t MF should be a better choice.

The increasing filtration rate with the increasing MF dosage might result from the fact that MF at high dosage flocculates particles more effectively than at small dosages.

The lower FMC achieved at 350 g/t A100 + 9.2 g/t MF than at 350 g/t A100 + 5.5 g/t MF and 350 g/t A100 + 18.3 g/t MF indicates the effect of MF on the solid hydrophobicity and total surface area. MF is hydrophilic in nature. At 5.5 g/t, MF adsorbed on solids weakens the solid hydrophobicity enhanced by A100. That is

why FMC of 350 g/t A100 + 5.5 g/t MF presents an average value between FMC of 350 g/t A100 and 5.5 g/t MF. At 350 g/t A100 + 9.2 g/t MF, MF flocculates the solid more effectively than at 5.5 g/t to produce bigger agglomerates while weakening the hydrophobicity enhanced by A100. The bigger agglomerates present smaller total surface area but weaker solid hydrophobicity when compared with that of 350 g/t A100 + 5.5 g/t MF. The competing effects between surface area and hydrophobicity on FMC led to an optimum dosage of MF. At this optimum dosage, A100 + MF produces a lowest FMC. Although increasing the MF dosage to 18.3 g/t increases the agglomerate size, leading to a higher U than that of lower dosage, this higher dosage of MF weakens the agglomerate hydrophobicity more strongly than lower dosage of MF in the combination of A100 + MF, producing agglomerates with lower surface hydrophobicity. The FMC with this dosage is higher than that at optimum dosage.

5.4. Zeta Potential Measurement

The zeta potential for blank and samples with A100, MF, and the combination of A100 and MF is shown in Figure 21 (Detailed data are listed in Table A2.3 in Appendix 2).

Clearly, filtration aid addition shows a marginal effect on zeta potential of solids,

all exhibiting a small negative zeta potential ranging from -5.5 mV to -8 mV.

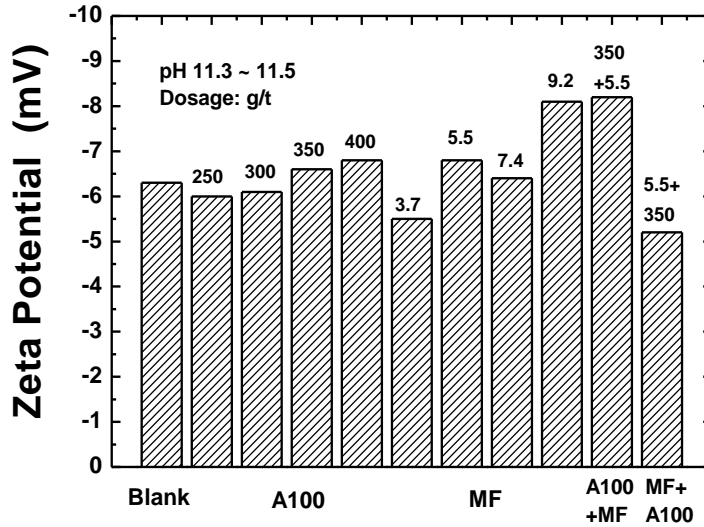


Figure 21. Effects of Filtration Aids Addition on Zeta Potential

The minor change of surface charge with the addition of filtration aids suggests that the surface charge does not play a significant role in governing the filtration performance in the current system.

5.5. Particle Size Distribution Measurement

The particle sizes measured for blank and samples with A100, MF, and the combination of A100 and MF are presented in Figure 22. d_{50} is used to

characterize the sample particle size. The detailed data are given in Table A2.4

Appendix 2.

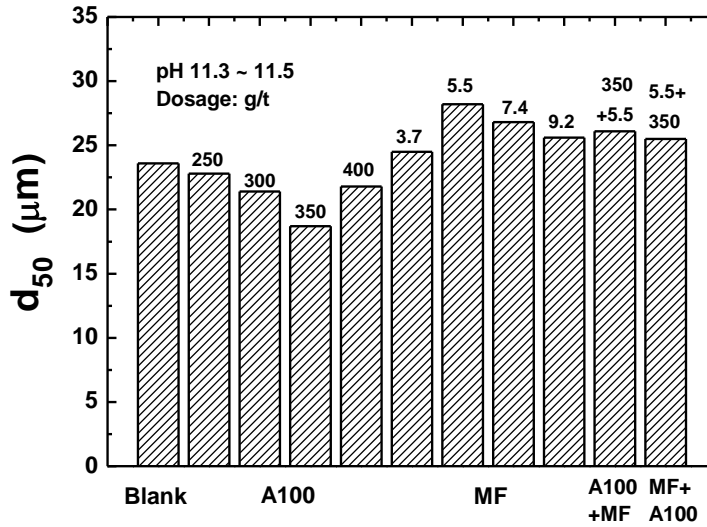


Figure 22. d_{50} of Sample with Filtration Aids Addition

Figure 22 shows that, among the filtration aids added, A100 could disperse the particles, rendering them smaller than the particle size of blank samples, while MF increases the aggregate size greatly. The combination of A100 and MF increases the aggregate size modestly compared with blank sample, but the aggregate size is smaller than that with MF used alone, demonstrating a trade-off effect between the effect of A100 and MF on aggregation.

The particle size distribution reflects the flocculation effectiveness of filtration

aids. MF, an effective flocculent, produces much bigger agglomerates than that of blank, while A100 disperses the sample, resulting in smaller particle size.

5.6. Effects of the Addition of Filtration Aids on Filtrate Viscosity

Figure 23 - 24 illustrate the filtration curves corresponding to 350 g/t A100 and 5.5 g/t MF samples for evaluating the effect of filtration aids addition on viscosity.

The cake filtration sections of the filtration curve in both cases are straight lines with an identical constant slope. This result indicates that the viscosity of the two filtrates is the same and constant during the filtration process. The results confirm that the effect of A100 and MF addition on filtrate viscosity is insignificant.

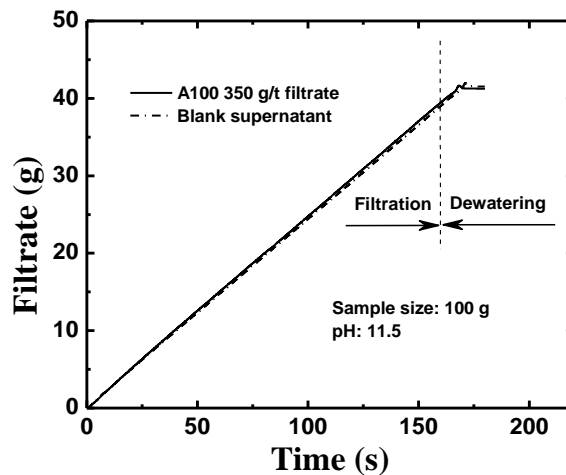


Figure 23. Effect of 350 g/t A100 Addition on Filtrate Viscosity

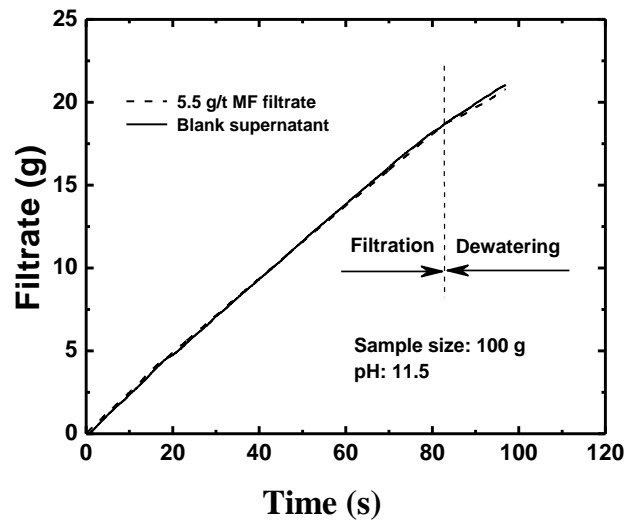


Figure 24. Effect of 5.5 g/t MF Addition on Filtrate Viscosity

5.7. Effects of the Addition of Filtration Aids on Surface Tension

The result in 5.6 (See Figure 23 - 24) could be used in this test again. The capillary dewatering sections of two filtration curves are both linear with similar constant slope $\frac{dm}{dt}$.

This finding suggests that the two liquids have similar surface tensions; the effect of addition of filtration aids on surface tension is insignificant. Therefore, the change of filtrate viscosity and surface tension caused by the addition of filtration aids is negligible in this study. The effect of this change on filtration performance is insignificant in this research.

To be effective, filtration aids added should adsorb onto the solid surface (Keller, et al, 1979). Above result might suggest that most of filtration aids added did not remain in the filtrate, but adsorbed onto the solid surface.

5.8. Saturated Cake Porosity and Permeability Measurement

The wet and dried cake from filtration tests is used to measure saturated cake porosity ϵ and permeability k_s . The $U - k_s$ correlation and $\epsilon - k_s$ correlation for tests with A100 and MF are shown in Figure 25 and Figure 26. The detailed data are given in Table A2.4 of Appendix 2.

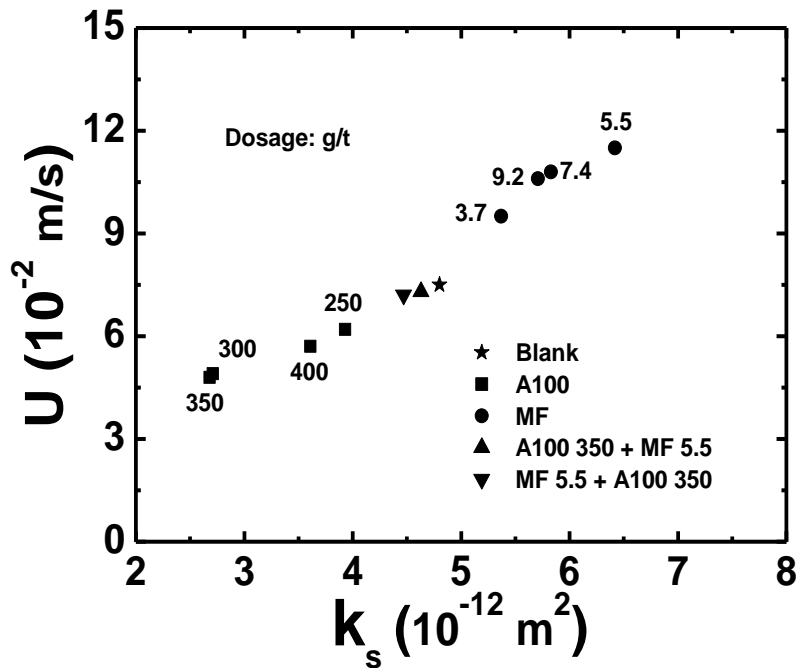


Figure 25. $U - k_s$ of Sample with A100 and MF Addition

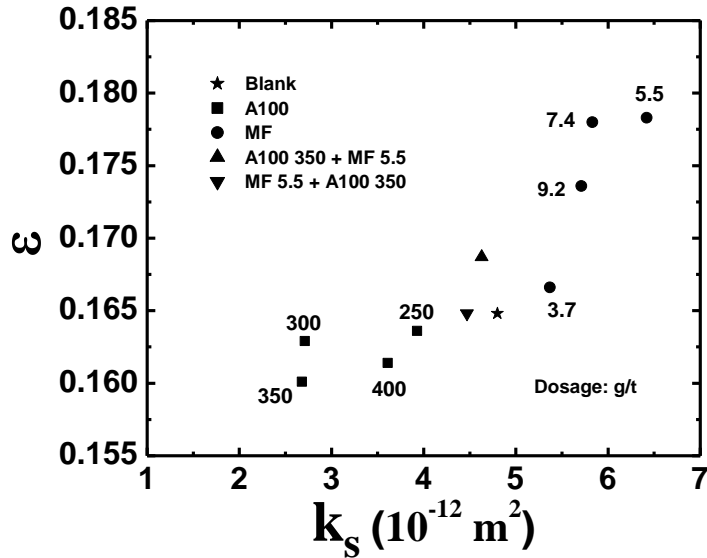


Figure 26. ϵ - k_s of Sample with A100 and MF Addition

The ϵ was measured directly from the cake, and the k_s was calculated from the filtration result. If the two interrelated parameters agree to each other, the result of two measurements would evaluate cake structure more effectively.

Figure 25 presents the correlation between U and k_s . It is evident that filtration rate U increases with the increase of cake permeability k_s , a clear linear relation exists between U and k_s . This finding agrees with the Darcy's law.

Figure 26 correlates ϵ with k_s . This correlation shows that ϵ increases with increasing k_s . This finding agrees to the established filtration theory that cake porosity is proportional to cake permeability.

The result in this test agrees with the results of the corresponding filtration rate obtained (see 5.2) and particle size measurement (see 5.5). Smaller particle with A100 addition produces a saturated cake with smaller porosity, permeability, and hence low filtration rate, while the bigger particle with MF addition produced a saturated cake of larger porosity, permeability, and hence a high filtration rate.

It was well known that larger saturated cake porosity and permeability correlate with coarser particle, and larger permeability correlates with higher U . The result above confirms this conclusion.

5.9. Initial Contact Angle Measurement

The dried cake from the filtration test was used to measure solid initial contact angle θ . The results are presented in Figure 27. The detailed data are given in Table A2.4 in Appendix 2.

The initial contact angle θ of filter cake solids produced by A100 and A100 + MF is bigger than that of blank, the θ obtained with MF and MF + A100 addition is similar to that of blank. The linear relation between SMC and θ suggested that SMC is largely determined by solid hydrophobicity.

Initial contact angle measurement suggests that A100 adsorption makes the solid surface more hydrophobic, and MF is ineffective in altering solid hydrophobicity.

The hydrophobicity enhanced by A100 increases with increasing A100 dosage until the dosage reaches 350 g/t. The hydrophobicity obtained by A100 + MF falls in between that obtained by A100 and by MF addition, while the hydrophobicity by MF + A100 addition is similar to that by MF addition. This result agrees with the filtration result.

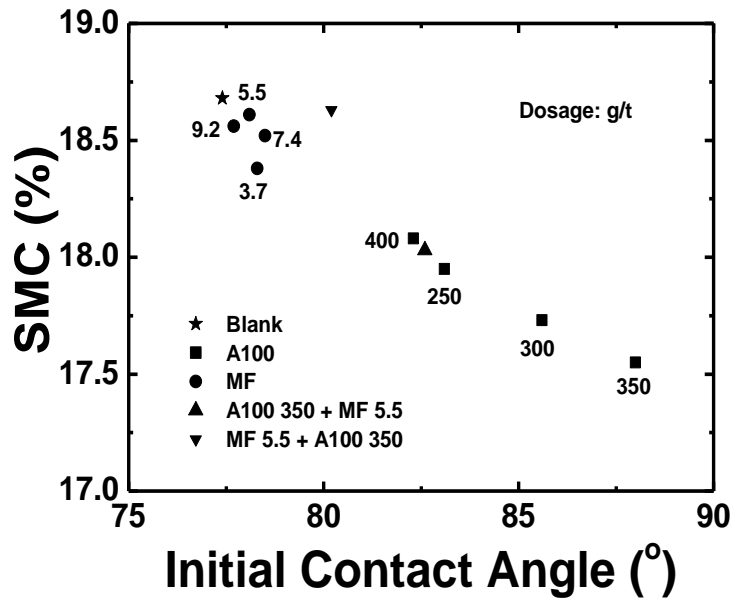


Figure 27. Initial Contact Angle with A100 and MF Addition

5.10. Backwashing

Figure 28 shows the FMC of cake backwashing with 7.5 g/t DAH solution.

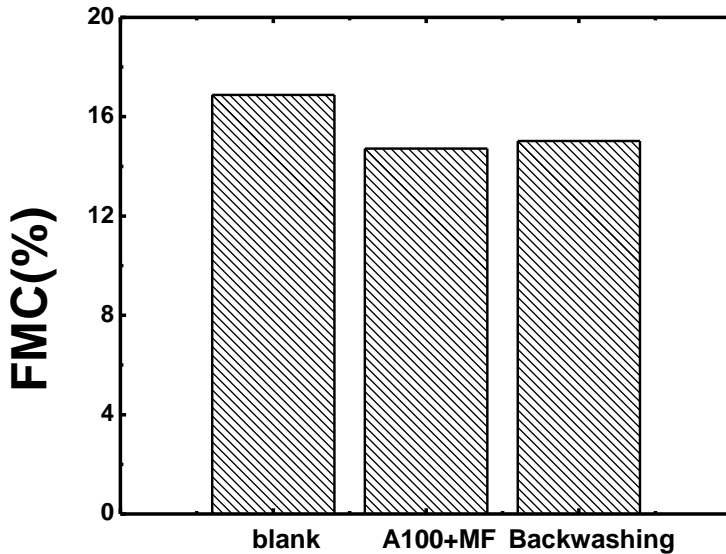


Figure 28. FMC of Cake Backwashing with 7.5 g/t DAH Addition

The result of this test shows that the backwashing with DAH does not improve the FMC. (Detailed data are given in Table A2.6 in Appendix 2, and related filtration curves are presented in Figure A3.11 of Appendix 3).

The ineffectiveness of cake backwashing with DAH might result from two reasons: either DAH does not adsorb onto the solid surface, or the adsorbed DAH is ineffective in improving solid hydrophobicity. In one hand, although solid surface was negatively charged, some Ca^{2+} ions adsorbed on particle surface after the bulk free water was removed resulted in strong positively charged patches on the solid surface. These positive patches prevented cationic DAH from adsorbing onto the solid surface. In the other hand, even the added DAH surfactant was

adsorbed onto the solid surface, it might not be so effective in enhancing the hydrophobicity of solid particles used in this study.

5.11. Filtration Aid Working Mechanism

5.11.1. Working Mechanism: A100

Based on the results shown in Figure 11 and Figure 12 in 5.2.1, A100 addition appears to decrease the aggregation size while increasing the solid surface hydrophobicity. To account for these results, the working model of A100 could be proposed to facilitate the understanding of the working mechanism of A100 in mineral slurry (shown in Figure 29).

A large amount of Ca^{2+} ions (see Table 1-2) in the blank slurry might induce coagulation of original negatively charged particles. Upon the addition of A100 ($\text{ROSO}_3^- \text{Na}^+$) into the slurry, mechanical stirring is applied to the slurry, which may break the association among particles, producing small particles with Ca^{2+} ions on its surfaces. Meanwhile, anionic functional group of A100 would adsorb onto solid surfaces through Ca^{2+} , with its hydrophobic tail extending to the surrounding water, making the particle more hydrophobic. The layer of A100 weakens the attraction force among particles forming a suspension of smaller

particles with more hydrophobic surface than that of blank. The particle size measured in 5.5 and initial contact angle measured in 5.9 confirm this hypothesis.

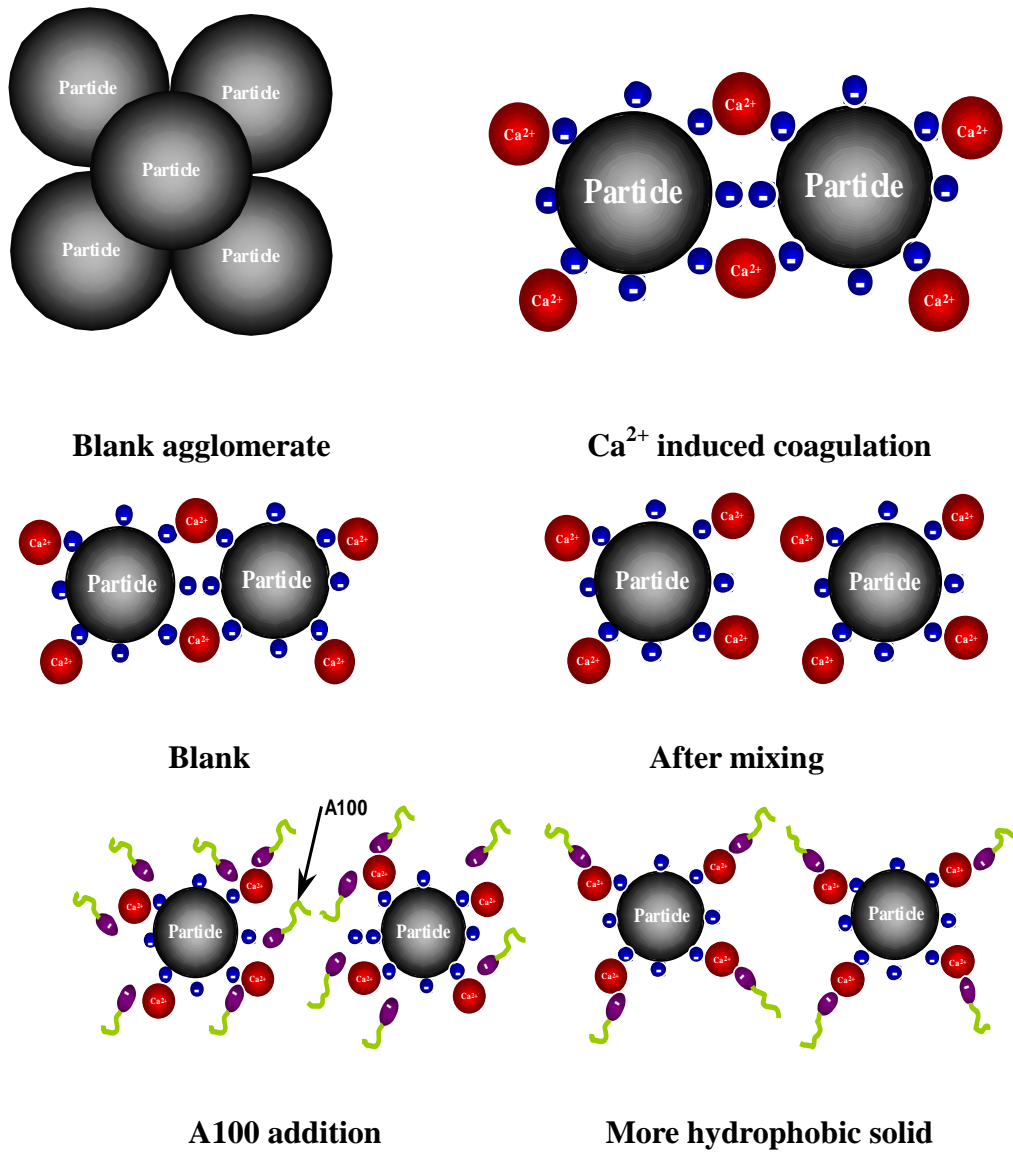


Figure 29. Working Mechanism of A100

5.11.2. Working Mechanisms: MF

Based on the results shown in Figure 14 and Figure 15 in 5.2.2, MF addition increases the aggregation size while it does not alter the surface hydrophobicity significantly. The working model of MF could be proposed in Figure 30.

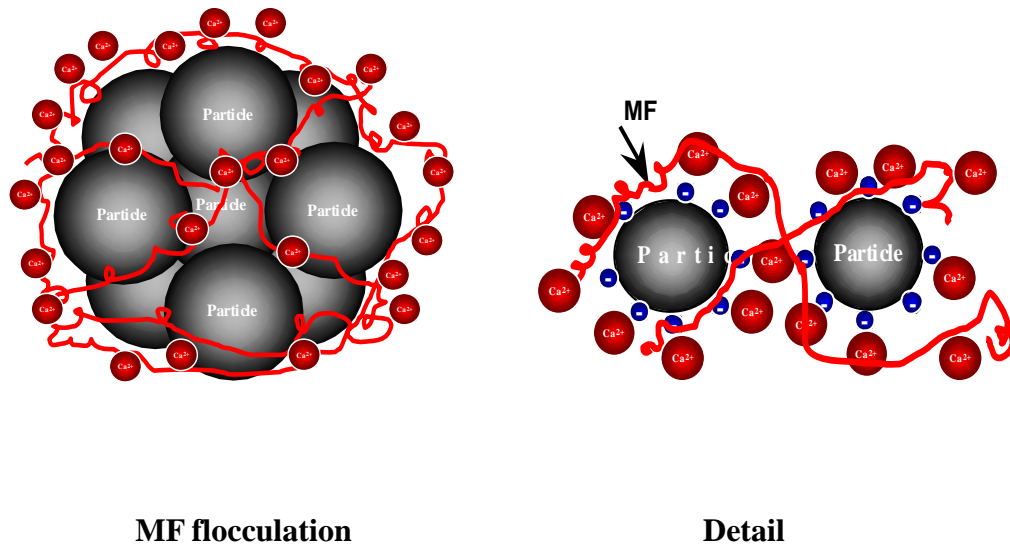


Figure 30. Working Mechanism of MF

Upon the addition of MF into blank slurry, the anionic functional group of MF attaches to solid surface in similar manner to that of A100, the long chain of MF is capable of bridging many particles to form larger flocs. The adsorption of MF (its hydrophobicity similar to that of solids in blank) does not significantly change the solid hydrophobicity, leading to similar SMC value. The particle size distribution measured in 5.5 and initial contact angle measured in 5.9 supports this hypothesis.

5.11.3. Working Mechanism: A100 and MF

The working model of A100 and MF addition is proposed in Figure 31 - 32.

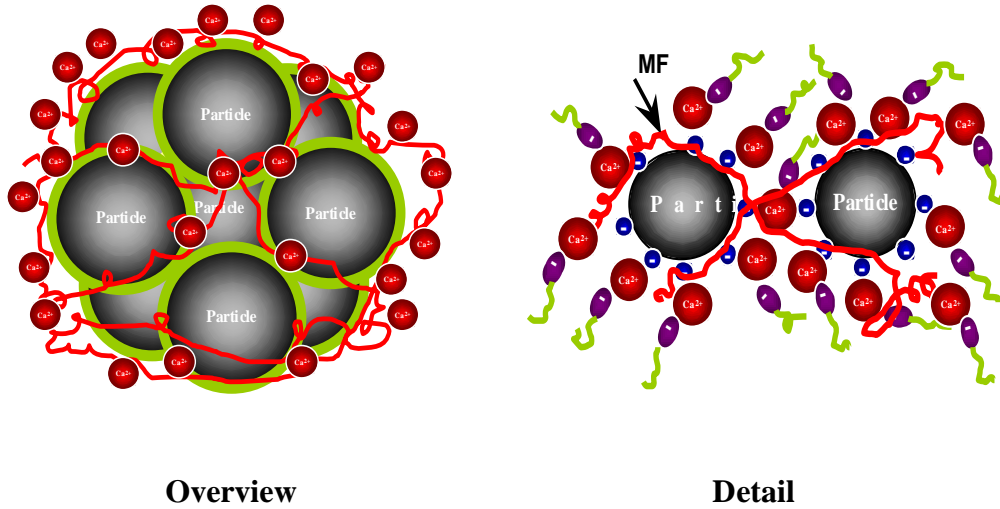


Figure 31. Working Mechanism of A100 + MF

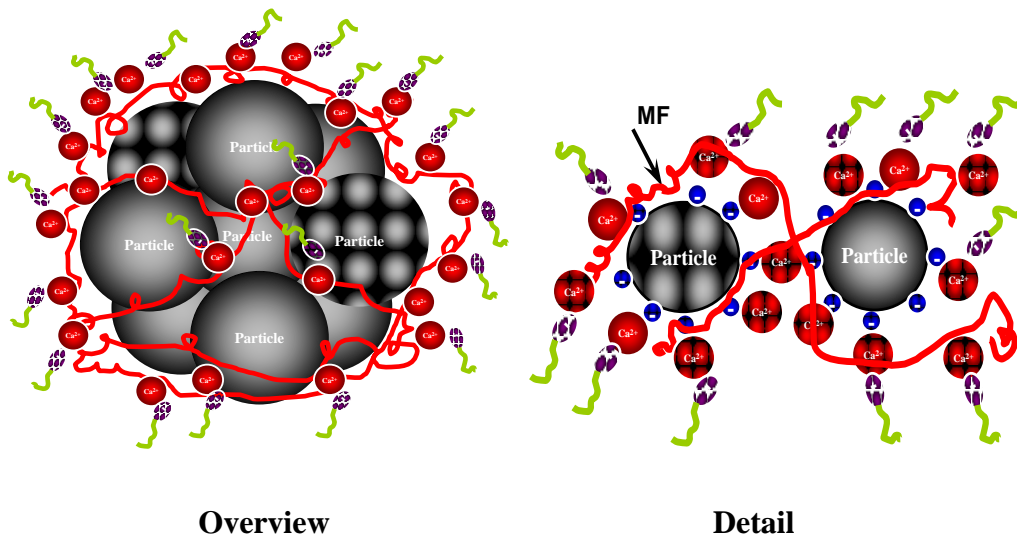


Figure 32. Working Mechanism of MF + A100

The results shown in Figure 17 and Figure 18 in 5.2.3 suggest that A100 and MF addition increases the aggregation size while the order of A100 and MF addition causes different impact on particle surface hydrophobicity.

When preparing the sample of A100 + MF, the addition of A100 works in the same manner as that described in section 5.11.1, increasing the solid hydrophobicity, the subsequent MF addition induces flocculation but reduces some degree of surface hydrophobicity due to the hydrophilic nature of MF. The overall effect is a trade-off between effects of two filtration aids. In general, A100 and MF together lead to an average filtration performance between that of A100 and MF, but much better than blank.

MF + A100 produces a higher FMC and a similar U comparing with that of A100 + MF. This might result from the fact that, in the case of A100 + MF, A100 added first alters the surface of every particle more hydrophobic, MF added later flocculates the solid adsorbed by A100; in the case of MF + A100, MF flocculates the particle first, forming bigger flocs with size similar to that with A100 + MF, the A100 added later only improves the outer surface hydrophobicity of the flocs; the particle surface within the flocs is not exposed to A100, and then its surface hydrophobic is not altered by A100. Because the total surface area of solid particles within the flocs is much larger than the outer surface area of the flocs,

the hydrophobicity of flocs with A100 + MF is much stronger than that with MF + A100. Therefore, A100 + MF produces lower FMC than MF + A100, but produces a similar U to that of MF + A100.

CHAPTER 6. CONCLUSIONS

The major findings derived from this study are summarized below.

- 1) For the Cu/Ni concentrate used in this study, it is hard for single filtration aid to improve both U and FMC simultaneously, but improving either U or FMC is relatively easy. Base on the filtration performance of each filtration aid, filtration aids tested are categorized into two types: the first type such as A100 achieves lower FMC, and the second type such as MF achieves higher U. The combination of A100 and MF at given dosages could achieve better performance than A100 and MF used alone. The optimum filtration performance is found at 350 g/t A100+ 9.2 g/t MF producing $U = 0.089$ m/s, $FMC = 12.76\%$, comparing with $U = 0.075$ /s, $FMC = 16.9\%$ for blank.
- 2) Interaction between A100 and MF in the combination of A100 + MF is significant for their filtration performance.
- 3) A100 disperses slurry but improves solid hydrophobicity, while MF flocculates the slurry but does not enhance solid hydrophobicity.

- 4) The assumption that good settling performance correlates with good filtration performance is inaccurate.
- 5) The effect of filtration aids on surface charge for the concentrate used in this study is insignificant.
- 6) Effect of filtration aids at the dosage used in this study on liquid viscosity and surface tension is insignificant.
- 7) There exist certain correlations among particle size, cake porosity and permeability, and filtration rate U : coarse particles correlate with bigger cake porosity and permeability, and higher U .
- 8) Cake backwashing with cationic surfactant DAH does not improve FMC.

CHAPTER 7. RECOMMENDATIONS

It is well known that pH of the mineral slurry plays an important role in achieving high efficient filtration. Upon the completion of this study, it was found that many filtration aids were pH sensitive. The pH of the mineral slurry used in this study is as high as around 12. Many filtration aids would either decompose or malfunction at this high pH condition. More efforts should be made to search for pH insensitive filtration aids.

It is believed that, during the filtration process, significant streaming potential arising from the capillary effect leads to a significant electroviscosity in addition to the conventional viscosity, which changes the actual viscosity greatly. In this study, little work was done to explore the impact of streaming potential on filtration performance. Therefore, further efforts should also be made to explore the effect of the streaming potential on the filtration efficiency.

BIBLIOGRAPHY

- Attia, Y. A. and S. Yu, "Flocculation and Filtration Dewatering of Coal Slurries Aided by Hydrophobic Polymeric Flocculant", *Separation Science and Technology*, 26(6), 816, 1991.
- Carman, P. C., "Some Physical Aspects of Water Flow in Porous Media", *Water Flow in Porous Media*, 74 – 75, 1948.
- Cheng, Y. S., Fang, S. R., Tierney, J. W. and S. H. Chiang, "Application of Enhanced Vacuum Filtration to Dewatering Fine Coal Refuse", *Separation Science and Technology*, 23 (12&13), 2113-2130, 1988.
- Geer, M. R., Jacobson, P. S. and H. F. Yancey, "Flocculation to Improve Coal Slurry Filtration", *Mining Engng.*, Vol. 11, 715-919, 1959.
- Keller, D. V., Jr., Stelma, G. J. and Y. M. Chi, "Surface Phenomena in Dewatering of Coal", EPA Report 600/7-79-008, 1979.
- Khandrika, S. M., Groppo, J. G. and B. K. Parekh, "Influence of Copper Ion Addition on Fine Coal Filter Cake Parameters", *Mineral and Metallurgical Processing*, 47, 1994.
- Morey, B., "Dewatering", *Kirk-Othmer Encyclopedia of Chemical Technology*, 7, 2000.
- Owen, M. J., "Enhancement of Mechanical Dewatering of Fine Coal by Surface-Active Additives", *Interfacial Phenomena in Coal Technology*, 169, 191 -192, 1985.
- Puttock, S. J., Fane, A. G., Fell, C. J. D., Robins, R. G. and M. S. Wainwright, "Vacuum Filtration and Dewatering of Alumina Trihydrate – the Role of Cake Porosity and Interfacial Phenomena", *International Journal of Mineral Processing*, 207, 1986.
- Singh, B. P., Besra, L., Reddy, P. S. R. and D. K. Sengupta, "Use of Surfactants to Aid the Dewatering of Fine Clean Coal", *Fuel* Vol. 77, No. 12, 1351, 1354, 1998.

- Svarovsky, L., "Filtration Fundamentals", Solid –Liquid Separation, 9, 171-192, 1977.
- Wakeman, R. J., "Cake Dewatering", Solid-liquid Separation, 305, 1977.
- Wheelock, T. D. and J. Drzymala, "Coal Hydrophobicity and its Role in Filtration and Dewatering", Proceedings of the Filtration Society, 351-353, 1991.
- Xu, Z., Zhou, Z., Liu, Q. and J. L. Yordan, "Role of Interfacial Phenomena in Fine Coal Dewatering", Processing of Hydrophobic Minerals and Fine Coal, Proceedings of the 1st UBC-McGill Bi-Annual International Symposium on Fundamental of Mineral Processing, 513, 514, 522, 1995.
- Yoon, R., Asmatulu, R., Yildirim, I., Jansen, W., Zhang, J., Atkinson, B. and J. Havens, "Development of Dewatering Aids for Minerals and Coal Fines", The Final Report to United States Department of Energy for Project Period During Jan. 2001 to Jan. 2004, 13, 2004.
- Yu, Z., "Flocculation, Hydrophobic Agglomeration and Filtration of Ultrafine Coal", Ph. D thesis, University of British Columbia, 49, 56-57, 71, 1998.

APPENDICES

1. Filtration Test Procedure

1.1. Sample Preparation

- 1) At the receiving of the sample, if not used immediately, it should be stored in a laboratory freezer set at $-18\text{ }^{\circ}\text{C}$ to keep the pH constant.
- 2) While homogenizing the original sample using a laboratory stirrer, effective sealing procedure should be applied to prevent the slurry from reacting with CO_2 in air, keeping the sample pH constant. The original solid content and the pH of the slurry are measured at this time.
- 3) According to the measured original solid content, the slurry solid content is adjusted to about 62.5% by removing supernatant of the slurry, if the solid content is lower than 62.5%, or by adding the original supernatant if the solid content is higher than 62.5%.
- 4) After the solid content of slurry is adjusted, the slurry is homogenized again. The thoroughly homogenized slurry is pumped via a peristaltic pump into a sample jar.
- 5) The sample in the jar is capped with Parafilm and stored in laboratory freezer until being used.

1.2. Conditioning

- 1) At the addition of filtration aid solution, the water contained in the solution should be counted into the slurry solid content to keep it around 62.5%.
- 2) The sample is placed on a mixer. The desired amount of filtration aid solution is added while mixing. Exposure of the sample to air should be avoided as much as possible to keep pH constant during the whole mixing process. Before and after the filtration aid solution added, the slurry pH is measured.

The mixing process lasts for 5 minutes: 4 minutes at 500 rpm, and then 1 minute at 300 rpm. A100 is added at the beginning of the mixing, and MF is added at the 4th minute; for the case of MF + A100, MF is added at the 3rd minute and then A100 is added.

- 3) Prior to filtration tests, it is important to ensure that the filtration press is dry and free of liquids that may be weighed in the sample.
- 4) Filter paper is placed in the filter press, which is then placed on a balance.

1.3. Computer Workstation

- 1) A clean, dry 100 ml graduated cylinder with a glass funnel is placed on the balance connected to the computer, which is then tared, the glass funnel is ensured to reach up and under the filter press spout.
- 2) The data acquisition software is started at this point.
- 3) The software comes up ready to read weights from the balance. Click on 'read data from balance.'
- 4) After the file table appears on the monitor, enter a file name for the test data downloadable to the Excel.
- 5) When the mixing is completed, the desired amount of sample slurry is transferred from the sample jar to the filter press placed on the balance. Then the filter press is positioned in the counter.
- 6) The cap is placed on the press and securely tightened down. Then the pressure is applied to the slurry in the filter press. The duration from the time at which the slurry is transferred into the press on the balance to the time when filtration starts in the counter should be controlled to about 30 seconds.
- 7) Click 'OK' on the computer and the programming is now running.
- 8) A preset pressure (15 psig) is applied to the filter system while the mass of the filtrate is read automatically as a function of filtration time.

- 9) The pressure is kept on for at least one minute past the evacuation of the bulk liquid (air pressure through spout, full cycle is 150 seconds).
- 10) The pressure on the press is released and the program is terminated.

1.4. Sample Treatment

- 1) The filter press is disassembled and the cake thickness is measured with the top to bottom of the empty press of 89 mm as the reference.
- 2) Place the wet cake onto a pre-weighed aluminium pan and weigh it.
- 3) Place the pan in an oven at 60°C for overnight.
- 4) The dried cake is taken out of the oven and placed in a desiccator to cool down to the room temperature for one hour.
- 5) Weigh the pan and the dry cake to calculate the solid content of the sample.
- 6) Data collected is converted from the mass of the filtrate into cake moisture content and the results are plotted for comparisons.

2. Results

Table A2.1. Original Concentrate Zeta Potential Measurement

Run	1	2	3	4	5	6	7	8	9	10	Ave
ζ (mV)	-5.2	-3.5	-8.5	-3.8	-7.9	-6.1	-10.8	-10.3	-3.4	-3.2	-1.80

Table A2.2. A100 and MF Settling Result

Time (min.)	Blank	250 g/t A100	300 g/t A100	350 g/t A100	400 g/t A100	1.9 g/t MF	3.7 g/t MF	5.5 g/t MF	7.4 g/t MF	MF +A100	A100 +MF
0	100	100	100	100	100	100	100	100	100	100	100
1	97.7	96	96	96	96.3	96	98	97	98	97	97
2	96.2	94.5	94.5	95	95	94	95	92.5	92.5	94	95
3	94.7	94	93	94	93	91	92	86	85	92	93
4	93.4	92.8	91.5	91	91	88.5	87	78.5	79	90	91
5	92	90.2	90	88.6	89.5	86	80	75	76	88	89
6	90.5	88.8	88.6	87	88	83	76	73	74	84	83
7	89.3	87.5	87	86	86.5	78	73	71.5	72	81	82
8	87.8	86	87	84.5	85	73	71.5	70	71	78	79
9	86.6	84.8	84.5	83	83.7	71	70	68.5	70	76	77
10	85.2	84	82.8	81.5	82.5	69	68.5	67.5	68.5	73	74
15	78.5	77	76	74.5	75	64	64	64	65	62	63
20	71.8	69.2	68.5	65.8	67	61.5	62	62	63	59	60
25	63.8	61.5	60	59	59	59.5	60	60	60.5	56	57
30	59.5	59	58	56.6	56.8	58	58.5	58.5	59	52.5	53

Table A2.3. Zeta Potential Measurement with Filtration Aids

Sample	Blank	250 g/t A100	300 g/t A100	350 g/t A100	400 g/t A100	350g/t A100 + 5.5 g/t MF
ζ (mV)	-6.3	-6.0	-6.1	-6.6	-6.8	-8.2
Sample	Blank	3.7 g/t MF	5.5 g/t MF	7.4 g/t MF	9.2 g/t MF	5.5 g/t MF + 350 g/t A100
ζ (mV)	-6.3	-5.5	-6.8	-6.4	-8.1	-5.2

Table A2.4. Filtration Test Result

Sample	U (m/s)	SMC (%)	ζ (mV)	d_{50} (μm)	Θ ($^{\circ}$)	ε	ρ (kg/m^3)	k_s (m^2)
Blank	0.075	18.68	-6.3	23.6	77.4	0.1648	4067	4.80E-12
250 g/t A100	0.062	17.95	-6	22.8	83.1	0.1636	4085	3.93E-12
300 g/t A100	0.043	17.73	-6.1	21.4	85.6	0.1629	4095	2.71E-12
350 g/t A100	0.041	17.55	-6.6	18.7	88	0.1601	4105	2.68E-12
400 g/t A100	0.057	18.08	-6.8	21.8	82.3	0.1614	4084	3.61E-12
3.7 g/t MF	0.095	18.38	-5.5	24.5	78.3	0.1666	4112	5.37E-12
5.5 g/t MF	0.115	18.61	-6.8	28.2	78.1	0.1783	4155	6.42E-12
7.4 g/t MF	0.108	18.52	-6.4	26.8	78.5	0.1780	4054	5.83E-12
9.2 g/t MF	0.106	18.56	-8.1	25.6	77.7	0.1736	3978	5.71E-12
350 g/t A100 + 5.5 g/t MF	0.072	18.03	-8.2	26.1	82.6	0.1687	4256	4.54E-12
5.5 g/t MF + 350 g/t A100	0.073	18.63	-5.2	25.5	80.2	0.1648	4574	4.56E-12

Table A2.5. Interaction Effect Test Result

Sample	300 g/t A100 + 5.5 g/t MF	350 g/t A100 + 5.5 g/t MF	400 g/t A100 + 5.5 g/t MF	350 g/t A100 + 9.2 g/t MF	350 g/t A100 + 18.3 g/t MF
U (m/s)	0.071	0.072	0.067	0.089	0.106
FMC (%)	14.44	14.46	14.69	12.76	14.29

Table A2.6. Backwashing Result

Sample	Blank	350 g/t A100 + 5.5 g/t MF	Backwashing with 7.5 g/t DAH
FMC (%)	16.88	14.72	15.02

3. Filtration Curves

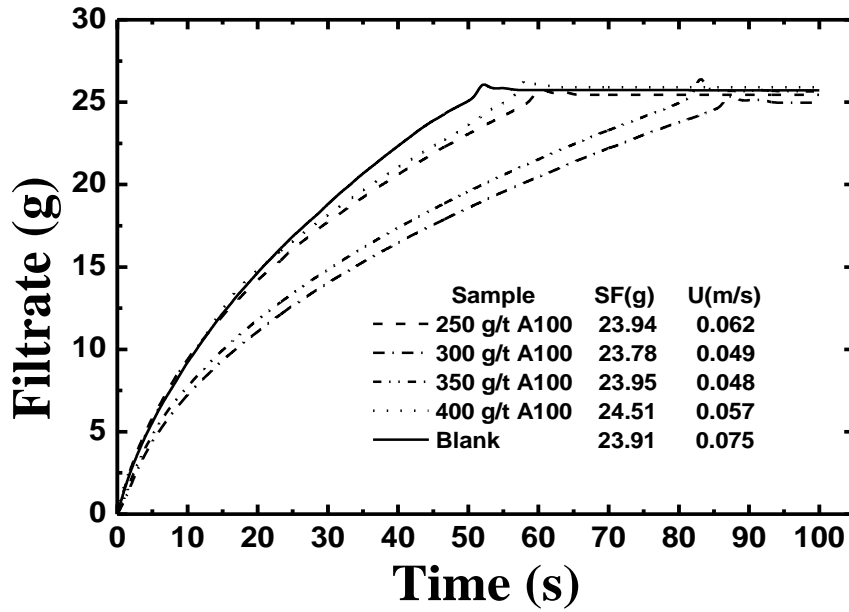


Figure A3.1. U with A100 Addition

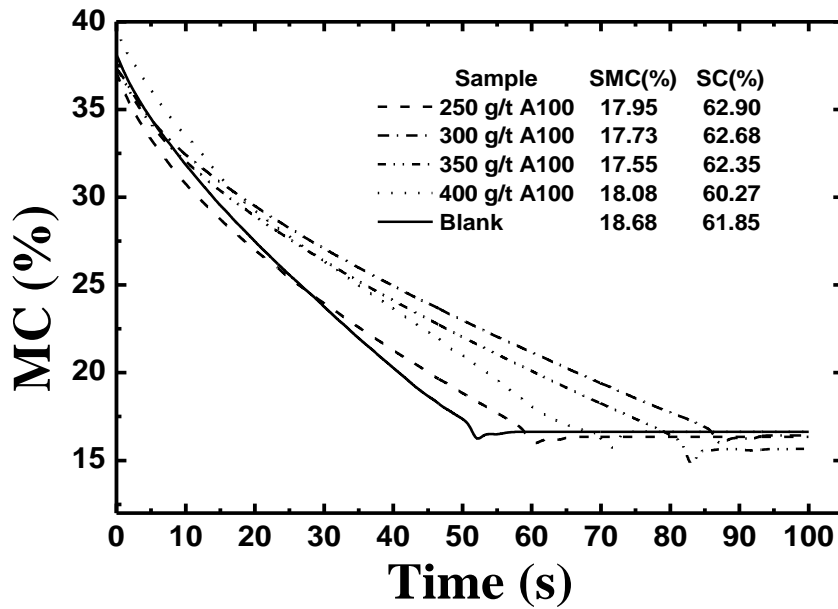


Figure A3.2. SMC with A100 Addition

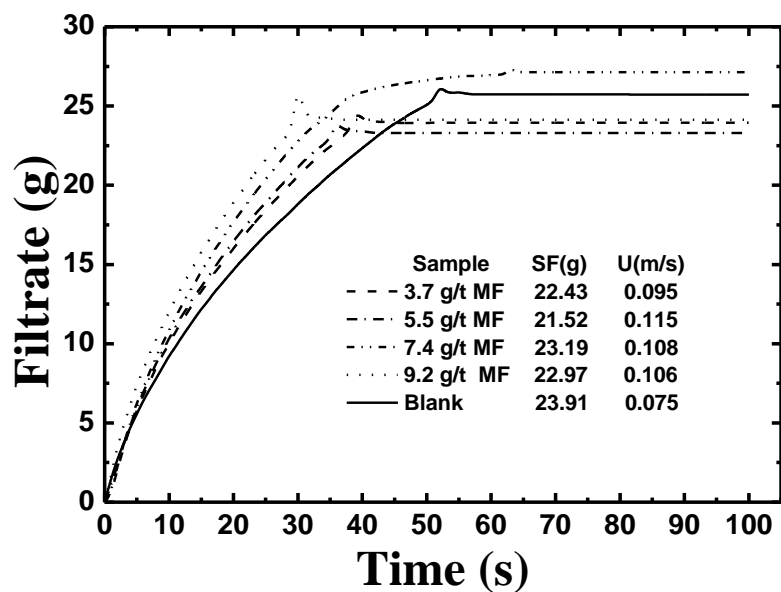


Figure A3.3. U with MF Addition

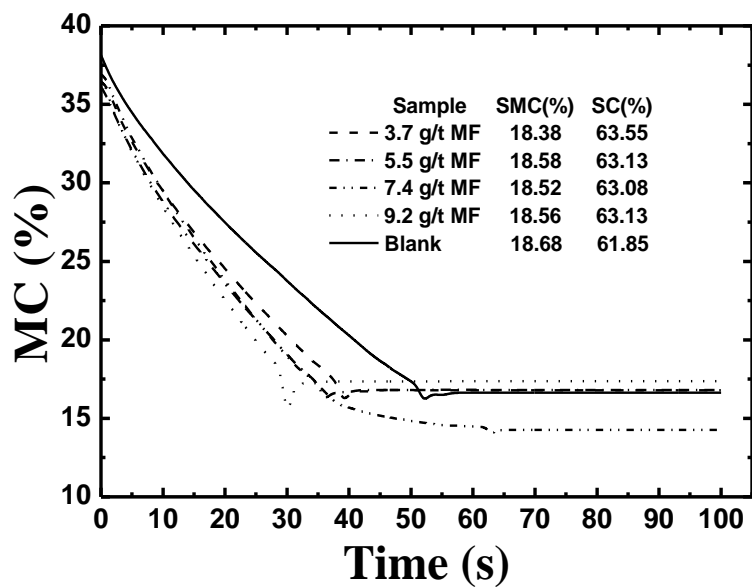


Figure A3.4. SMC with MF Addition

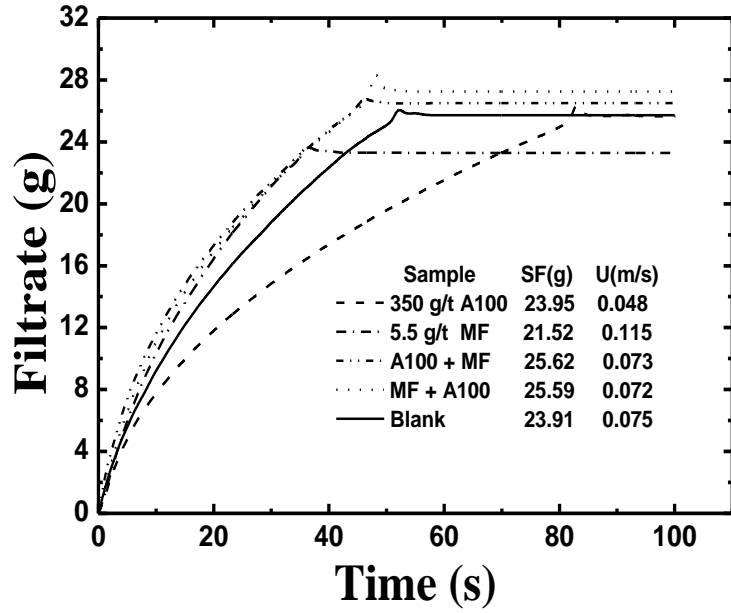


Figure A3.5. U with A100 & MF Addition

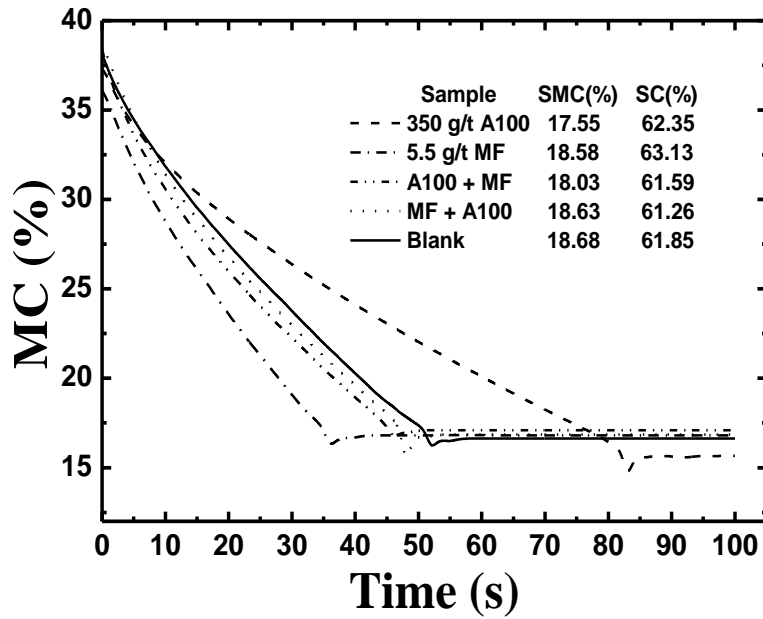


Figure A3.6. SMC with A100 & MF Addition

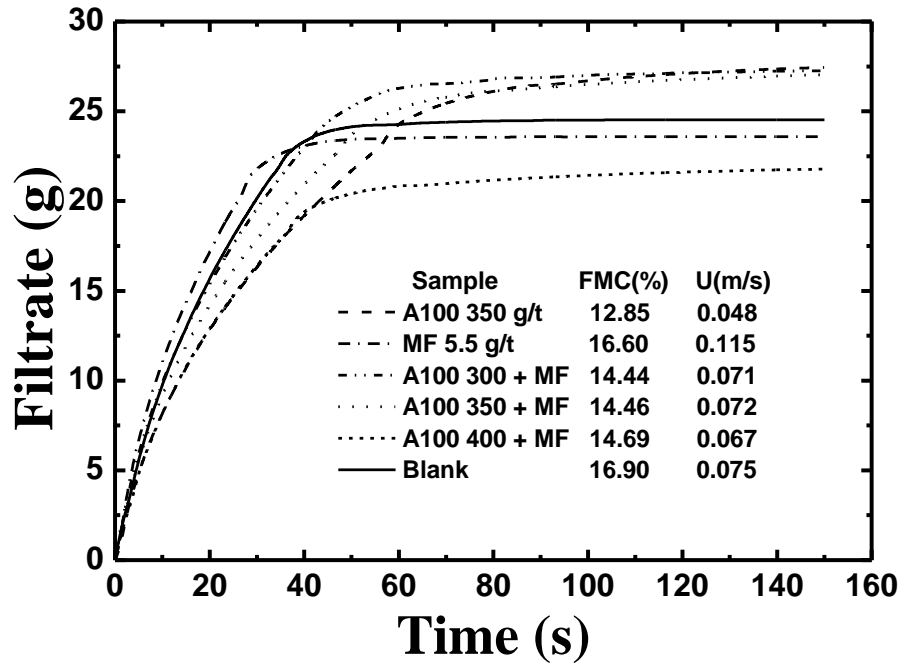


Figure A3.7. U of x g/t A100 + 5.5 g/t MF Addition

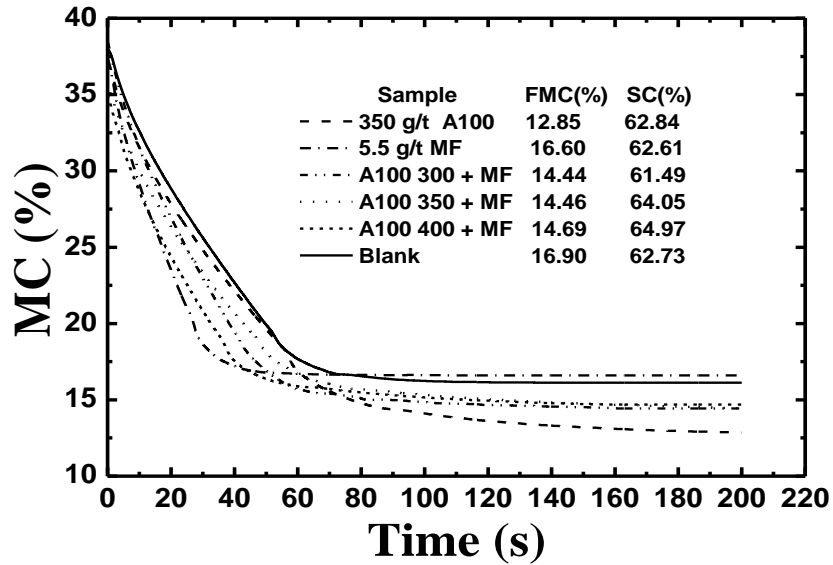


Figure A3.8. FMC of x g/t A100 + 5.5 g/t MF Addition

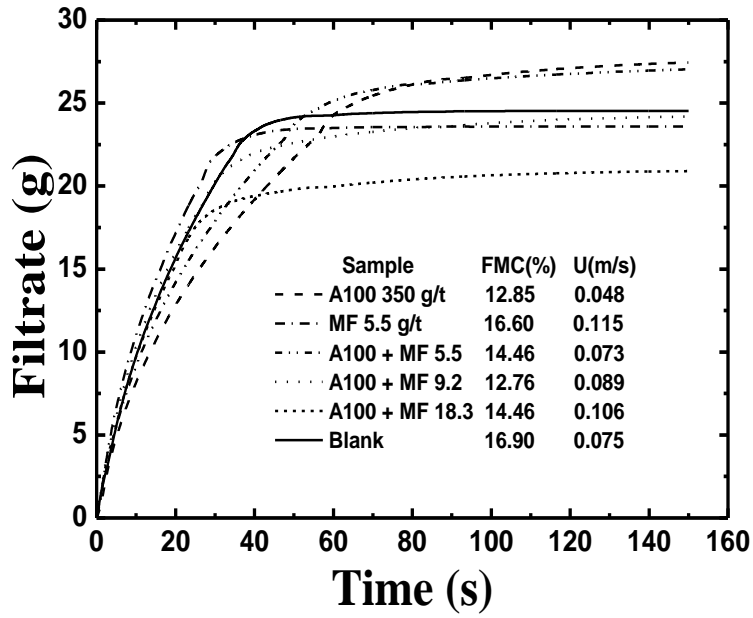


Figure A3.9. U of 350 g/t A100 + y g/t MF Addition

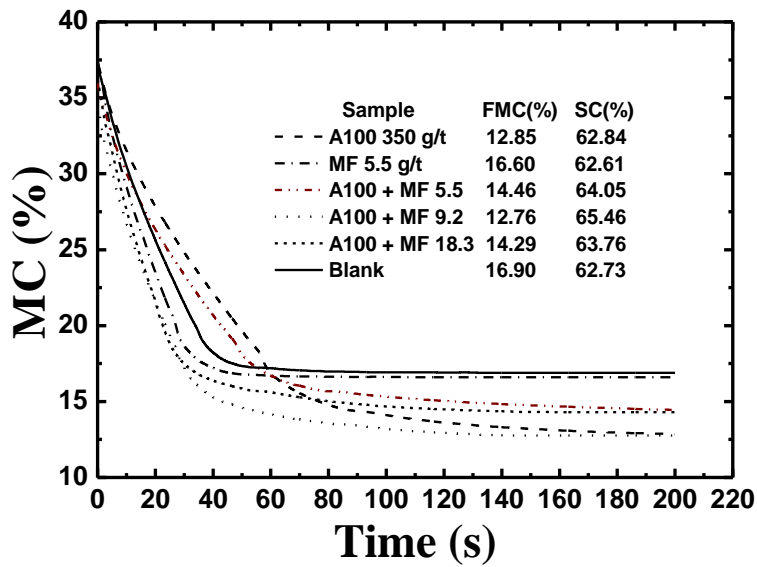


Figure A3.10. FMC of 350 g/t A100 + y g/t MF Addition

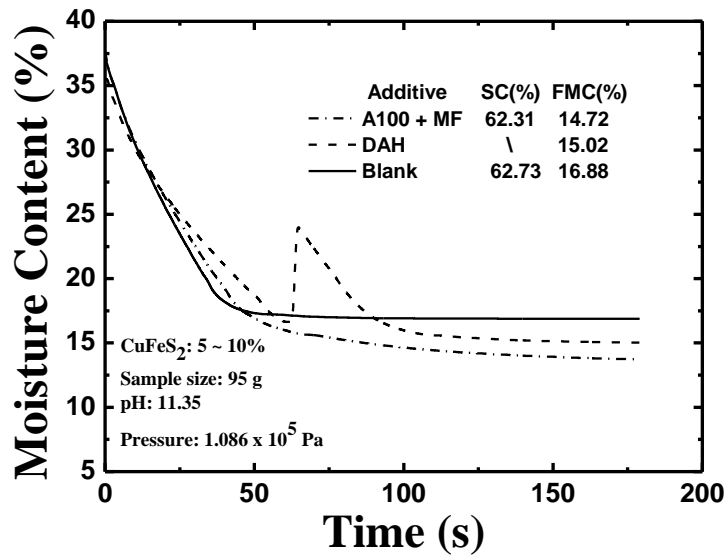


Figure A3.11. Moisture Content Curve of Cake Backwashing with 7.5 g/t DAH Addition

4. Table of Test Points

Table A4.1. Settling Test Points

Sample	Dosage (g/t)
A100	250, 300, 350, 400
MF	3.7, 5.5, 7.4, 9.2
350 g/t A100 + 5.5 g/t MF	√
5.5 g/t MF + 350 g/t A100	√
Blank	√

Table A4.2. Filtration Test Points

Sample	Dosage (g/t)
A100	250, 300, 350, 400
MF	3.7, 5.5, 7.4, 9.2
x g/t A100 + 5.5 g/t MF	300, 350, 400
350 g/t A100 + y g/t MF	5.5, 9.2, 18.3
5.5 g/t MF + 350 g/t A100	√
Blank	√

Note: √ test done